Loss of Rap1 supports recombination-based telomere maintenance independent of RNA-DNA hybrids in fission yeast

Yan Hu[1], Henrietta W. Bennett[1,3], Na Liu[1], Martin Moravec[2], Jessica F. Williams[1], Claus M. Azzalin[2,4], and Megan C. King[1#]

[1] Department of Cell Biology, Yale School of Medicine, 333 Cedar Street, New Haven, CT, 06520-8002, USA
[2] Institute of Biochemistry (IBC), Eidgenössische Technische Hochschule Zürich (ETHZ), Zürich, CH-8093, Switzerland
[3] Current affiliation: Stanford University School of Medicine, Stanford, California, 94305-5441, USA
[4] Current affiliation: Instituto de Medicina Moleculare, Lisboa, Portugal

[#] Corresponding author: megan.king@yale.edu, tel: +1 2037374628

Running Title: Telomerase- and hybrid-independent survivors

Character Count: 38,382 (excluding Methods and References)

Keywords: telomere / recombination / RNA-DNA hybrid / TERRA / shelterin / ALT pathway

Abstract

To investigate the molecular changes needed for cells to maintain their telomeres by recombination, we monitored telomere appearance during serial culture of fission yeast cells lacking the telomerase recruitment factor Ccq1. Rad52 is loaded onto critically short telomeres shortly after germination despite continued telomere erosion, suggesting that recruitment of recombination factors is not sufficient to maintain telomeres in the absence of telomerase function. Instead, survivor formation coincides with the derepression of telomeric repeat-containing RNA (TERRA). Degradation of telomere-associated TERRA in this context drives a severe growth crisis, ultimately leading to a distinct type of linear survivor with altered cytological telomere characteristics and the eviction of the shelterin component Rap1 (but not the TRF1/TRF2 orthologue, Taz1) from the telomere. We demonstrate that deletion of Rap1 is protective, preventing the growth crisis that is otherwise triggered by degradation of telomere-engaged TERRA in survivors with linear chromosomes. Thus, modulating the stoichiometry of shelterin components appears to support recombination-dependent survivors to persist in the absence of telomere-engaged TERRA.

Introduction

Telomeres are specialized nucleoprotein structures at the ends of linear eukaryotic chromosomes. Telomeres protect the chromosome ends from degradation, aberrant recombination and end-to-end fusions (DE LANGE 2009; DEHE AND COOPER 2010), while also supporting the formation of heterochromatin at chromosome ends (BUHLER AND GASSER 2009). Telomeric DNA consists of tandem double-stranded G-rich repeats and a single-stranded 3' overhang (BLACKBURN 1991). The 3' ssDNA overhang is sequestered by engaging in higher-order structures in part due to the binding of sequence-specific telomeric binding proteins (BLACKBURN 2001). In at least some organisms, the telomere binding protein TRF2 drives formation of a structure called a "t-loop"; TRF2 is a component of the shelterin complex that includes the additional factors TRF1, RAP1, TIN2, TPP1 and POT1 in mammalian cells (DE LANGE 2005). The fission yeast (*S. pombe*) genome encodes several classes of telomere binding proteins, many of which are orthologous to mammalian shelterin components. For example, Taz1 (related to mammalian TRF1/TRF2) recognizes dsDNA telomere repeats (COOPER *et al.* 1997), while the conserved Pot1 specifically recognizes the 3' ssDNA G-rich overhang repeat (BAUMANN AND CECH 2001). These modules are bridged by the shelterin components Rap1, Poz1 and Tpz1; Rap1 constitutes the binding interface with Taz1 (CHIKASHIGE AND HIRAOKA 2001; KANOH AND ISHIKAWA 2001). Taz1 and Pot1 contribute to negative and positive regulation of telomerase recruitment, respectively (COOPER *et al.* 1997; BAUMANN AND CECH 2001). Pot1 is also thought to protect the telomere from degradation, as acute loss of Pot1 function in fission yeast leads to rapid, extensive telomere loss through 5' end resection (PITT AND COOPER 2010).

In fission yeast, telomeric DNA is composed of several 100 bps of degenerate $GG_{1\text{-}5}$TTAC[A] repeats (COOPER AND HIRAOKA 2006). Telomeric sequence can be lost through two primary mechanisms. The first is the so-called "end replication problem", which arises from the inability of lagging strand synthesis to replicate the chromosome in its entirety. This leads to telomere shortening concomitant with each cell division. The second is degradation, caused by nucleases when they have access to the telomere (SHORE AND BIANCHI 2009; LONGHESE *et al.* 2010). The primary mechanism to counteract telomere loss is the action of the reverse transcriptase telomerase, which is preferentially recruited to short telomeres (TEIXEIRA *et al.* 2004; NANDAKUMAR AND CECH 2013). The fission yeast telomerase is comprised of the conserved catalytic subunit Trt1, the RNA component TER1 that encodes the template for addition of the degenerate telomeric repeat to support telomere elongation, the conserved subunit Est1, and accessory factors such as the Lsm proteins (NAKAMURA *et al.* 1997; BEERNINK *et al.* 2003; LEONARDI *et al.* 2008; WEBB AND ZAKIAN 2008; TANG *et al.* 2012). In fission yeast, the factor Ccq1 links telomerase recruitment to the 3' telomeric overhang through Tpz1 and Pot1 to support telomere maintenance (MIYOSHI *et al.* 2008; TOMITA AND COOPER 2008).

Somatic mammalian cells do not express telomerase at sustained levels mostly due to transcriptional silencing of the catalytic subunit TERT (KIM *et al.* 1994; WRIGHT *et al.* 1996), and therefore can undergo a limited number of cell divisions before critically short telomeres drive cell cycle arrest and senescence or apoptosis. Thus, cancer cells typically harbor mutations that lead to reactivation of TERT transcription (KIM *et al.* 1994; SHAY AND BACCHETTI 1997; HEIDENREICH AND KUMAR 2017). However, in about 15% of cancer cells, the alternative lengthening of telomeres (ALT) pathway can instead support telomere maintenance, a process accomplished by homologous recombination (HR) (CESARE AND REDDEL 2010; APTE AND

COOPER 2017). The ability of cells to adapt mechanisms to maintain their telomeres through recombination to compensate for loss of telomerase activity was first discovered in budding yeast (LUNDBLAD AND BLACKBURN 1993). In fission yeast lacking the telomerase-recruitment factor Ccq1, telomeres gradually shorten with increasing passage number, eventually leading to a growth crisis; the "survivors" that emerge from this crisis can utilize recombination to maintain their telomeres (MIYOSHI *et al.* 2008; TOMITA AND COOPER 2008). Fission yeast cells can also survive complete telomere loss by circularization of each of their three chromosomes (NAKAMURA *et al.* 1998). The generation of these "circular survivors" can occur through multiple pathways, including single-strand annealing, which is independent of HR (WANG AND BAUMANN 2008).

Despite the heterochromatic nature of chromosome ends, eukaryotic telomeres are transcribed into a group of long non-coding RNA species (AZZALIN *et al.* 2007; LUKE *et al.* 2008; SCHOEFTNER AND BLASCO 2008; BAH *et al.* 2012). The transcription of TElomeric Repeat-containing RNA (TERRA) is evolutionarily conserved, and has been suggested to function in the homeostasis of telomere length regulation, heterochromatin establishment, and telomeric HR (BAH AND AZZALIN 2012; AZZALIN AND LINGNER 2015; RIPPE AND LUKE 2015). TERRA transcription is largely RNA Pol II-dependent, is initiated at subtelomeric region(s) and proceeds towards the 3' end of the telomeric tract (BAH AND AZZALIN 2012). The majority of TERRA molecules are shorter than 500 base pairs (bps) in fission yeast cells, whereas in mammalian cells TERRA can be as long as several kilobases (AZZALIN *et al.* 2007; SCHOEFTNER AND BLASCO 2008; FEUERHAHN *et al.* 2010; BAH *et al.* 2012; GREENWOOD AND COOPER 2012). The steady-state level of TERRA levels is negatively regulated by Taz1 and Rap1 in fission yeast, being very low in wild-type cells (BAH *et al.* 2012; GREENWOOD AND COOPER 2012).

Studies both in human and fission yeast cells demonstrate that TERRA molecules localize primarily within the nucleus, and partially colocalize with telomeres (SCHOEFTNER AND BLASCO 2008; BAH *et al.* 2012; CUSANELLI *et al.* 2013). A fraction of TERRA molecules are 3' polyadenylated (AZZALIN AND LINGNER 2008; SCHOEFTNER AND BLASCO 2008; BAH *et al.* 2012; PORRO *et al.* 2014). Poly(A)- and poly(A)+ TERRA have different subnuclear distributions: the majority of poly(A)- TERRA associates with telomeric DNA, whereas poly(A)+ TERRA is mostly released from telomeres and is instead present throughout the nucleoplasm (PORRO *et al.* 2014; MORAVEC *et al.* 2016). We recently reported that telomere shortening in fission yeast leads to derepression of TERRA, similar to what has been observed in budding yeast (CUSANELLI *et al.* 2013; MORAVEC *et al.* 2016). A substantial fraction of this telomere shortening-induced TERRA is polyadenylated and physically interacts with telomerase, thus promoting its recruitment to the telomere (MORAVEC *et al.* 2016), potentially in a manner specific to the telomere from which the TERRA was transcribed (CUSANELLI *et al.* 2013). Interestingly, polyadenylation of fission yeast TERRA occurs coincident with 3' RNA cleavage at sites that lead to loss of nearly the entire G-rich telomere tract (MORAVEC *et al.* 2016). Therefore, at least in WT fission yeast, only the poly(A)- TERRA carries G-rich telomeric repeat sequences. Taken together, these observations raise the possibility that nascent, telomere-associated TERRA includes the telomeric repeats, but that upon maturation and release from the telomeres, the telomeric-repeat tract is lost. To date the impact of telomere-associated TERRA on telomere maintenance by recombination in the absence of telomerase function in cycling cells has gone largely uninvestigated in fission yeast, although recent evidence suggests that TERRA up-regulation in quiescent fission yeast correlates with increased telomere rearrangements driven by RNA-DNA hybrids and recombination (MAESTRONI *et al.* 2017).

G-rich TERRA can form RNA-DNA hybrids at the telomere, resulting in a triple-stranded structure called an “R-loop”; R-loops are antagonized by the activity of RNase H, which specifically degrades RNA engaged in such hybrids (BALK *et al.* 2013; ARORA *et al.* 2014; BALK *et al.* 2014). Recent evidence indicates that telomeric R-loops may actively engage in HR in telomerase-negative human and yeast cells. For example, depletion of RNase H1 (alone or in combination with RNase H2) results in accumulated RNA-DNA hybrids at telomeres and greater telomere recombination in *cis*, while RNase H over-expression leads to decreased telomere recombination in pre-senescent cells and compromised telomere maintenance in ALT cells (BALK *et al.* 2013; ARORA *et al.* 2014; BALK *et al.* 2014).

In order to test the consequences of TERRA up-regulation, several studies have taken advantage of engineered, inducible promoters at a TERRA transcriptional start site to construct a transcriptionally inducible telomere (tiTEL) (MAICHER *et al.* 2012; PFEIFFER AND LINGNER 2012; ARORA *et al.* 2014; MORAVEC *et al.* 2016), which can increase telomeric RNA-DNA hybrids (ARORA *et al.* 2014). However, the strong transcription driven by a heterologous promoter may also disrupt the heterochromatic state of telomeres and influence the maturation, turnover and function of natural TERRA molecules. Despite the growing evidence linking TERRA to regulation of telomeric recombination, it is still not clear how endogenous TERRA (and natively-formed telomeric RNA-DNA hybrids) might be altered to promote telomere recombination and formation of telomerase-deficient survivors in an unperturbed system. Further, the proteins that physically associate with TERRA, and the potential role(s) that these interactions play in telomere maintenance, are still poorly understood. In human cells, it has been suggested that the heterogeneous nuclear protein A1 (hnRNPA1) and shelterin component TRF2 bind TERRA, regulating telomere end protection during cell cycle progression and heterochromatin formation at telomeres, respectively (DENG *et al.* 2009; FLYNN *et al.* 2011; PORRO *et al.* 2014).

Here, we show that an increase in TERRA levels occurs during the emergence of linear, recombination-based survivors in fission yeast. TERRA induction promotes a transition to productive telomere maintenance by engaging in RNA-DNA hybrids at the telomere(s). Constitutive degradation of RNA-DNA hybrids drives these linear survivors back into a growth crisis, from which an alternative type of linear survivor arises. Surprisingly, the telomeres in these RNase H-resistant survivors no longer recruit Rap1 despite enhanced Taz1 binding. Importantly, deletion of Rap1 insulates linear survivors from the crisis induced by RNA-DNA hybrid degradation, suggesting that this altered telomere composition functionally promotes telomere maintenance in the absence of telomere-associated TERRA.

Results

Recombination likely precedes the growth crisis in *ccq1Δ* cells

As a model system for recombination-based telomere maintenance, we chose to take advantage of *S. pombe* lacking Ccq1, which is necessary for recruitment of telomerase to the telomeres and also suppresses the DNA damage checkpoint (TOMITA AND COOPER 2008). It is well-established that serially cultured cells lacking Ccq1 undergo a growth crisis due to telomere erosion; the subsequent survivors that emerge in *ccq1Δ* liquid cultures maintain linear chromosomes through recombination, although survivors that have circularized all three of their chromosomes have also been observed, particularly when propagated on (non-competitive) solid media (MIYOSHI *et al.* 2008; TOMITA AND COOPER 2008). Immediately following germination, *ccq1Δ* cells propagated in liquid culture grow slightly slower than WT cells (Fig. 1A). During serial culturing, *ccq1Δ* cells undergo a growth crisis after approximately 80 generations, which is followed by the emergence of survivors that have growth rates similar to the starting population, consistent with earlier studies (MIYOSHI *et al.* 2008; TOMITA AND COOPER 2008) (Fig. 1A). To quantitatively measure telomere length in the population of cells, we used TeloPCR-seq, a PacBio approach that we developed and employed previously (BENNETT *et al.* 2016; MORAVEC *et al.* 2016). We compared telomere length in a WT cell population (see also (BENNETT *et al.* 2016)) and *ccq1Δ* cells at three time points: as early as possible after germination (Day 1, estimated to be 28 generations based on single colony size before inoculation of clonal liquid cultures; green arrow), at the depth of the *ccq1Δ* crisis (Day 8, 81 generations; red arrow) and the survivors (Day 30, >250 generations; purple arrow). The telomeric repeat tract of amplified telomeres in *ccq1Δ* cells was much shorter than in WT cells soon after germination (mean length of 88 bps, Fig. 1B). During the crisis amplified telomeres further shortened to an average of 55 bps, although this value may overestimate telomeric repeat length as our telomere analysis pipeline requires the presence of the extreme 3' subtelomeric sequence, which could be lost from very short telomeres (BENNETT *et al.* 2016). *ccq1Δ* survivors possess substantially longer telomeric repeat tracts, averaging 117 bps, although they remain shorter than WT telomeres.

Consistent with previous studies in budding yeast (ABDALLAH *et al.* 2009; KHADAROO *et al.* 2009), these observations suggest that pre-senescent *ccq1Δ* cells have undergone substantial telomere loss before entering a growth crisis (Fig. 1A,B). Moreover, this interpretation is consistent with the activation of the ATR-dependent Chk1 checkpoint (TOMITA AND COOPER 2008) and formation of Crb2 foci (CARNEIRO *et al.* 2010) in early generation *ccq1Δ* cells. In light of these results, we were curious if telomere recombination was occurring shortly after germination, but was insufficient to maintain telomere length. To assess this, we serially cultured cells lacking both Ccq1 and Rad55/Rhp55, which ultimately survive primarily through chromosome circularization (MIYOSHI *et al.* 2008). Consistent with our hypothesis and the observed role for the recombination factor Rad52 in antagonizing senescence in budding yeast models of telomere dysfunction (LUNDBLAD AND BLACKBURN 1993; ABDALLAH *et al.* 2009), *ccq1Δ*/*rad55Δ* cells grow much more poorly than *ccq1Δ* cells immediately following germination (Fig. 1A), suggesting that the activation of recombination at critically short or deprotected telomeres occurs early after germination of *ccq1Δ* cells; indeed, recombination appears to support improved cell growth but is insufficient to maintain telomere length. Shortly after germination of *ccq1Δ* cells (approximately 28 generations) we observe Rad52(Rad22)-mCherry foci in 64% of *ccq1Δ* cells (n=233) compared to only 2% of WT cells (n=239) (Fig. 1C). While

only a subset of these foci colocalize with Taz1-GFP (22% of *ccq1Δ* cells; Fig. 1C), it is likely that the Rad52-mCherry foci that do not colocalize with Taz1-GFP correspond to critically short telomeres that are no longer competent to recruit sufficient Taz1 to be visualized. Indeed, the percentage of cells with 2-3 Taz1-GFP foci decreases from about 85% for WT cells to only 30% of *ccq1Δ* cells, while instead nearly 70% of *ccq1Δ* cells have 0-1 Taz1-GFP foci (compared to only about 10% of WT cells; Fig. 1D). Taken together, these results suggest that recombination is active at *ccq1Δ* telomeres shortly after germination. However, these observations also highlight that the ability of telomeres to engage recombination factors is not sufficient to maintain telomeres, suggesting that an additional factor(s) underlies the ability of cells to productively use recombination to maintaining their telomeres, as seen in survivors.

Increased telomere-associated Taz1 in *ccq1Δ* survivors

To begin to investigate what other factors might influence recombination-based telomere maintenance to support survivor formation, we monitored the cytological appearance of telomeres during the serial culturing of *ccq1Δ* cells. To this end, we carried out growth assays on WT and *ccq1Δ* cells expressing Taz1-GFP from its endogenous locus and visualized telomeres at each day for over twenty days (>250 generations). Expression of Taz1-GFP caused slight suppression of the severity of the growth crisis seen in *ccq1Δ* cells (Supplemental Fig. S1A), likely because of a mild loss of function phenotype ((TUZON *et al.* 2004; SUBRAMANIAN *et al.* 2008) and see more, below). However, the *ccq1Δ* growth crisis and the emergence of survivors is preserved in Taz1-GFP expressing cells as assessed by monitoring both cell length, which correlates with checkpoint arrest, and telomere length by EcoRI digestion of genomic DNA followed by Southern blotting (Fig. 2A-B). As has been described previously (TOMITA AND COOPER 2008), *ccq1Δ* survivors (with and without Taz1-GFP expression) undergo telomere rearrangements leading to the appearance of a larger, EcoRI-liberated fragment that is detected with telomere probes (asterisk in Fig. 2B).

Early after germination, telomeres in WT and *ccq1Δ* cells appear qualitatively similar, with a variable number of telomere bundles (about 2-4) per cell clustered at the nuclear periphery; the limits of the nuclear compartment can be discerned by the faint, diffuse nucleoplasmic Taz1-GFP signal (Figure 2C). During the growth crisis in *ccq1Δ* cells around 150 generations, Taz1-GFP foci are much fainter than in WT cells, and indeed are undetectable in some cells (Fig. 2C, asterisk). Further, in some cases telomeres appear declustered and are more interiorly localized within the nuclear volume (Figure 2C, arrow). Taz1-GFP in *ccq1Δ* survivors recovered its focal nature, although the number and localization of the foci varied widely within the population (Fig. 2C). Surprisingly, using identical image acquisition and image processing conditions, the total focal Taz1-GFP intensity in *ccq1Δ* survivors is increased compared to WT cells (Fig. 2C-D). In addition, many *ccq1*Δ survivors have only one, very bright Taz1-GFP focus (Fig. 2C, arrowhead); these bright foci undergo dramatic declustering during mitosis when they appear to resolve into individual telomeres (Supplemental Fig. 1B). To examine whether the changes in Taz1-GFP appearance were due to changes in the spatial distribution of focal Taz1 (i.e. increased telomere clustering) or reflect altered Taz1-GFP recruitment to the telomeres, we measured the total GFP intensity per Taz1 focus from summed intensity projections (see Experimental Procedures). In WT cells, the intensity of Taz1-GFP foci (per cell) remained largely constant over the growth assay (Fig. 2D), while in *ccq1Δ* cells, focal Taz1 intensity is lost as cells undergo telomere shortening and enter into the growth crisis (Fig. 2D). However, during the emergence of survivors beginning at 167 generations, fluorescence intensity far surpasses the

mean total focal intensity seen in WT cells (Fig. 2D). Critically, we observe the same trend if we integrate GFP at the Taz1 locus after the emergence of *ccq1Δ* survivors (Fig. 2E), verifying that expression of Taz1-GFP during serial culturing is not a driver of this phenotype.

Increased TERRA transcription drives Taz1-GFP accumulation at telomeres

In budding yeast, short telomeres preferentially up-regulate expression of TERRA and show increased telomeric RNA-DNA hybrids (GRAF *et al.* 2017), which is suggested to drive HR at the shortest telomeres (TEIXEIRA *et al.* 2004; FALLET *et al.* 2014). Given the suggestion that the Taz1 orthologue TRF2 binds to TERRA in mammalian cells (DENG *et al.* 2009), we investigated whether TERRA up-regulation is tied to the increased recruitment of Taz1-GFP to telomeres in *ccq1Δ* survivors. Treatment of cells with the histone deacetylase inhibitor Trichostatin A has been shown to increase TERRA production in *S. pombe* (MORAVEC *et al.* 2016). We recapitulated these findings (Supplemental Fig. S2A) and found that TSA treatment was sufficient to increase the intensity of Taz1-GFP at telomeric foci (Fig. 3A). Because TSA treatment broadly impacts chromatin state, we also tested whether an increase in TERRA driven by a synthetic transcriptionally-inducible telomere (MORAVEC *et al.* 2016) is sufficient to increase Taz1-GFP recruitment to the telomere. Over four or six days of TERRA induction from a single telomere in a strain expressing Taz1-GFP, we observed a modest but statistically significant increase in Taz1-GFP intensity (Fig. 3B); the more muted increase in Taz1-GFP intensity observed using the tiTEL system compared to TSA treatment (or that seen in *ccq1Δ* survivor cells) is consistent with the expression of TERRA from a single telomere in the tiTEL system. To further probe this model, we examined how degradation of RNA-DNA hybrids, which we expect to release at least a fraction of telomere-associated TERRA, impacts the recruitment of Taz1-GFP under conditions of TERRA up-regulation. To this end, we integrated the inducible nmt41 promoter in front of the Rnh201 gene, which encodes an RNase H2 homologue capable of digesting RNA specifically engaged in RNA-DNA hybrids and TERRA in budding yeast when overexpressed (HUERTAS AND AGUILERA 2003; EL HAGE *et al.* 2010; BALK *et al.* 2013); we found that Rnh201 over-expression (Supplemental Fig. S2B-C) is sufficient to suppress telomeric RNA-DNA hybrids in *S. pombe* by DNA-IP using the S9.6 antibody, which specifically recognizes RNA-DNA hybrids (Supplemental Fig. S2D). Interestingly, over-expression of Rnh201 largely prevented the TSA-dependent increase in Taz1-GFP recruitment to telomeres (Fig. 3C), supporting a role for nascent or otherwise DNA-engaged G-rich TERRA in recruitment of Taz1-GFP in addition to the binding of Taz1 to the dsDNA telomeric tract.

TERRA levels increase in recombination-based survivors, but driving TERRA production cannot prevent telomere crisis in pre-senescent *ccq1Δ* cells

Studies in both budding yeast and human cells suggest that TERRA up-regulation underlies productive recombination to maintain telomeres in the absence of telomerase, which correlates with elevated levels of telomeric RNA-DNA hybrids (ARORA *et al.* 2012; BALK *et al.* 2013; YU *et al.* 2014; GRAF *et al.* 2017). Consistent with these observations, TERRA levels, which are already ~10-fold higher in *ccq1Δ* cells shortly after germination than WT cells, are dramatically increased in *ccq1Δ* survivors irrespective of whether Taz1-GFP was expressed during serial culturing (Fig. 3D). Indeed, the progressive increase in TERRA levels during the emergence of *ccq1Δ* survivors as detected by quantitative RT-PCR (Fig. 3E) correlates temporally with both improved growth and the observed increase in Taz1-GFP intensity (Fig. 2C-D). Moreover, we detected an increase in telomeric RNA-DNA hybrids by DNA-IP/qRT-PCR in *ccq1Δ* survivors (Fig. 3F). We were also curious whether TERRA levels increase in survivors derived from other

genetic backgrounds. Consistent with the ability of TERRA to support ongoing telomeric recombination in budding yeast (BALK *et al.* 2013), we observe mild TERRA induction in recombination-competent *trt1Δ* survivors, which when serially cultured in liquid media likely contain both linear and circular types of survivors (NAKAMURA *et al.* 1998) (Supplemental Fig. S2E). By contrast, although *ccq1Δ/rad55Δ* cells show very high levels of TERRA shortly after germination (at 38 generations), *ccq1Δ/rad55Δ* survivors have nearly undetectable TERRA levels, far below what is seen in WT cells, likely due to complete loss of telomeric repeats (Figure 3G). Taken together, these results suggest that cells lacking Ccq1 have higher levels of TERRA shortly after germination. Further, during formation of survivors, TERRA production either continues to increase (in *ccq1Δ* recombination-competent strains) or is lost (in recombination-deficient genetic backgrounds that undergo chromosome circularization such as *ccq1Δ/rad55Δ*).

Our data suggest that TERRA up-regulation during the emergence of survivors from the growth crisis in *ccq1Δ* cells supports recombination-based telomere maintenance. However, we were curious whether driving TERRA production from the time of germination would be sufficient to avoid the growth crisis in *ccq1Δ* cells altogether. To examine this, we again took advantage of the tiTEL system. Shortly after germination, *ccq1Δ* tiTEL cells serially restruck on plates under conditions of TERRA induction grew much more slowly than *ccq1Δ* cells or tiTEL cells grown under the same conditions (Fig. 3H). Similarly, upon serial culturing we find that *ccq1Δ* tiTEL cells grow more poorly than *ccq1Δ* cells shortly after germination, display a more severe growth crisis, but ultimately form survivors (Fig. 3I). Interestingly, we find that Rad52-mCherry is enriched on telomeres one day after tiTEL induction (but not in cells in which the tiTEL was repressed), consistent with signals that slow cell growth (Fig. 3J). Thus, while we observe that TERRA levels increase during the formation of *ccq1Δ* linear survivors, engineered TERRA over-expression cannot overcome the passage of cells through a period of catastrophic growth crisis.

Degradation of RNA-DNA hybrids drives *ccq1Δ* survivors to enter a second growth crisis from which new survivors emerge

We observe that TERRA levels increase in *ccq1Δ* survivors coincident with the enhanced recruitment of Taz1-GFP to the telomere. To further test whether TERRA (and specifically TERRA engaged in RNA-DNA hybrids) is responsible for this increase in Taz1-GFP recruitment, we over-expressed Rnh201 in this genetic background. Strikingly, after over-expression of Rnh201 for 16 hours (Supplemental Fig. S3A), the intensity of Taz1 foci in *ccq1Δ* survivor cells reverted to levels below WT (Fig. 4A and Supplemental Fig. S3B), thereby correlating with telomere length in this population (Fig. 1B). Given that TERRA production and Taz1-GFP intensity at the telomeres increase during survivor emergence (Figs. 2C-D and Fig. 3D), we next asked if degradation of telomeric RNA-DNA hybrids (Supplemental Fig. S2D) impacts the growth rate of *ccq1Δ* survivors. Indeed, induction of Rnh201 caused *ccq1Δ* survivors to rapidly reenter a growth crisis (Fig. 4B-C). Ultimately “new” survivors emerged about 50 generations after Rnh201 induction (Fig. 4B-C) despite persistent expression of Rnh201 (Supplemental Fig. S3A). Despite the constitutive degradation of RNA-DNA hybrids (Supplemental Fig. S2D), these “new” survivor cells, which we term RNase H2-resistant (RHR) *ccq1Δ* survivors, maintain linear telomeres as revealed by Southern blot (Fig. 4D). Fission yeast with circularized chromosomes are highly sensitive to the genotoxin MMS (REF and Fig. 4E, *trt1Δ*O), while those with linear chromosomes are not (Fig. 4E, *ccqΔ*L). The relative insensitivity of RHR survivors compared to established strains with circular chromosomes suggests that they are linear (Fig. 4E).

RHR *ccq1Δ* survivors display altered recruitment of telomere binding proteins and compartmentalization of telomeres

To gain further insights into the mechanisms that RHR *ccq1Δ* survivors employ to maintain telomeres, we once again visualized telomeres by expression of Taz1-GFP. Despite the initial drop in Taz1-GFP recruitment after critical RNA-DNA hybrid degradation (Fig. 4A), the generation of RHR survivors over 15 days of serial culturing led to a recovery of high Taz1-GFP levels at the telomeres, similar to our observation for the initial *ccq1Δ* survivors (Fig. 5A-B). Moreover, the appearance of telomeres as visualized by expression of Taz1-GFP was substantially altered, with abundant declustered, expanded telomeric foci (Fig. 5A. right panel). To further quantitate this defect, we took advantage of an image analysis pipeline we initially developed to render and measure the size of heterochromatin foci in fission yeast (SCHREINER *et al.* 2015). In WT cells, the true size of telomere clusters is nearly always smaller than the diffraction limit of our microscope, and thus they appear equivalent to the point spread function (PSF; Fig. 5C-D). The mean size of the Taz1-associated telomere clusters in the initial *ccq1Δ* survivors is greater than the PSF (Fig. 5C-D); this cannot solely be explained by a decrease in telomere foci number (and therefore an increase in the number of telomeres residing in the same focus; Fig. S1C). However, the telomere foci in the RHR *ccq1Δ* survivors are highly expanded (Fig. 5C) and irregularly shaped (Fig. 5D), suggestive of telomere declustering and/or decompaction. Culturing of *ccq1Δ* cells under constitutive Rnh201 over-expression from the time of germination also led to formation of linear survivors with telomeres that cytologically resembled the RHR *ccq1Δ* survivors selected after initial *ccq1Δ* survivor formation (Supplemental Figs. S3D).

Telomere declustering has been observed in a number of contexts; in budding yeast telomere clustering is influenced by telomere binding proteins, including Rap1, which serves to recruit Sir3, which is in turn critical for telomere clustering (GOTTA *et al.* 1996; RUAULT *et al.* 2011; HOZE *et al.* 2013). In WT cells over-expressing Rnh201, Rap1-GFP typically localizes to 2-3 telomere clusters per cell as for Taz1-GFP (Fig. 6A-B and Supplemental Fig. S1C); we observe similar Rap1 appearance in WT cells or initial *ccq1Δ* survivors (Supplemental Fig. S4A-B). However, in stark contrast to the increase in Taz1-GFP recruitment in RHR *ccq1Δ* survivors, there is a profound loss of Rap1-GFP from RHR *ccq1Δ* survivor telomeres (Fig. 6A). Indeed, in 45% of cells we could not detect any Rap1-GFP telomere recruitment, while 2 or more Rap1-GFP associated telomere clusters were seen only very rarely (Fig. 6B). Chromatin immunoprecipitation followed by qPCR further validated this observation, as we find a significant decrease in the association of Rap1-GFP with the subtelomere upon long-term Rnh201 over-expression specifically in *ccq1Δ* survivors (Fig. 6C). Thus, although Rap1 and Taz1 recruitment is often thought to be tightly coupled (MILLER *et al.* 2005), in RHR survivors their telomere association becomes uncoupled. To gain further insights into the mechanisms at play we measured the expression of both Taz1 and Rap1. At the protein level, we find that Taz1 is increased in *ccq1Δ* survivors (whether derived in the absence or presence of the GFP tag) and is maintained in RHR *ccq1Δ* survivors (Fig. 6D), suggesting that enhanced expression may support the elevated levels of Taz1-GFP at the telomere in both types of survivors. By contrast, Rap1 expression levels remain nearly constant in all conditions (Fig. 6D), arguing that altered recruitment, not a loss of expression, underlies the loss of Rap1 from the telomere.

The growth crisis induced by RNA-DNA hybrid degradation can be circumvented by deletion of Rap1

The loss of Rap1 from the telomere of RHR *ccq1Δ* survivors (but not initial *ccq1Δ* survivors) suggests that Rap1 may negatively influence TERRA-independent telomere maintenance by recombination. To test this hypothesis, we compared the growth response of *ccq1Δ* survivors to critical Rnh201 over-expression in the presence and absence of Rap1 (Fig. 6E). We carried out serial culturing of *ccq1Δ* nmt41-Rnh201 and *ccq1Δ rap1Δ* nmt41-Rnh201 cells under three conditions: constitutive Rnh201 repression (black, in the presence of thiamine), constitutive Rnh201 over-expression (OE; light grey circles) and switching from repression (13 days) to over-expression (arrow, dark grey diamonds). Consistent with Figure 4, critical induction of Rnh201 in *ccq1Δ* cells at day 13 leads to a growth crisis (days 14-19), followed by recovery at day 20 to achieve a growth rate similar to cells cultured under conditions of constitutive Rnh201 over-expression. By contrast, critical Rnh201 over-expression in cells lacking Rap1 at day 13 led to a growth rate identical to cells under constitutive Rnh201 over-expression essentially immediately, without a growth crisis (Fig. 6E). It has long been established that deletion of Rap1 leads to telomere elongation in telomerase-positive fission yeast cells (KANOH AND ISHIKAWA 2001), which is tied to enhanced recruitment of telomerase to the telomere (DEHE *et al.* 2012). We therefore addressed the possibility that loss of Rap1 is able to compensate for defective telomerase recruitment in the absence of Ccq1, thereby supporting the growth of RHR *ccq1Δ* survivors through a telomerase-dependent mechanism. However, we find that deletion of the essential telomerase component Est1 has no effect on the growth of RHR *ccq1Δ* survivors (Supplemental Fig. S4D), arguing that telomere maintenance in this context remains telomerase-independent. Thus, Rap1 appears to attenuate productive, TERRA-independent telomere recombination. How RHR *ccq1Δ* survivors displace Rap1 from the telomere despite its continued expression (Fig. 6D) and the persistence of the Rap1-binding partner, telomeric Taz1 (Figs. 4 and 5), will require further study, although these observations suggest that the Taz1-Rap1 binding interface is subject to modulation.

Discussion

Here we find that loss of the telomerase recruitment factor Ccq1 leads to progressive telomere shortening despite loading of Rad52 onto telomeres prior to substantial growth arrest, suggesting that additional factors are required for recombination to productively lengthen telomeres. We provide evidence that the spontaneous increase of telomere-associated, telomeric repeat-containing RNA (TERRA) is a critical factor in the transition to productive telomere maintenance by recombination. The "active" form of TERRA in this pathway appears to be engaged in RNA-DNA hybrids, driving different consequences in telomerase-deficient cells depending on the telomere state. In pre-senescent cells, increased telomere-associated TERRA is detrimental and telomere recombination is inefficient. By contrast, during survivor emergence, TERRA levels increase spontaneously (and/or are selected for during competition in liquid culture); this TERRA is harnessed to promote efficient telomere recombination and telomere elongation. Long-term degradation of telomeric RNA-DNA hybrids compromises the growth of *ccq1Δ* survivors, ultimately leading to a new survivor type with altered biochemical and cytological characteristics. These RHR *ccq1Δ* survivors are characterized by loss of telomeric Rap1; deletion of Rap1 is sufficient to avoid the growth crisis induced upon RNA-DNA hybrid degradation in *ccq1Δ* survivors, suggesting that TERRA-independent recombination pathways can be accessed to maintain telomeres by recombination.

A switch from telomerase to recombination

As we place increased accumulation of telomere-associated TERRA as a key step in the transition to productive recombination, we favor a model, consistent with previous studies, in which changes to chromatin state within the subtelomere occur upon telomere shortening, supporting derepression of TERRA (RIPPE AND LUKE 2015; MORAVEC *et al.* 2016). Indeed, induction of TERRA has been suggested to occur as part of the more global loss of the telomere position effect upon telomere shortening (MANDELL *et al.* 2005; ARNOULT *et al.* 2012; CUSANELLI *et al.* 2013). Further, depletion of the histone chaperone ASF1 can induce a switch to the ALT pathway, suggesting that changes in the chromatin landscape are sufficient to activate recombination-based telomere maintenance (O'SULLIVAN *et al.* 2014). Ccq1 also contributes to recruitment of the SHREC complex to telomeres to promote heterochromatization (Sugiyama *et al.*, 2007) and mutations of Ccq1 that alter the checkpoint response but do not compromise SHREC recruitment drive survivors that undergo chromosome circularization rather than maintenance of linear chromosomes by recombination (MOSER *et al.* 2011). Combined with the observation that TERRA levels begin to increase early after germination in cells lacking Ccq1 (Fig. 3F), these data suggest that the combination of a more transcriptionally permissive chromatin state combined with shortened telomeres (GRAF *et al.* 2017) together drives high levels of TERRA, consistent with the ability of this genetic background to maintain linear chromosomes via recombination (MIYOSHI *et al.* 2008; TOMITA AND COOPER 2008). Within this context, the slow emergence of survivors over many generations could reflect transmissibility of heterochromatic marks at the subtelomere and/or the requirement for additional changes, for example to checkpoint signaling, that remain to be uncovered.

Support of recombination by telomere-associated TERRA

When telomere-associated TERRA is degraded, post-senescent *ccq1Δ* survivors reenter a growth crisis (Fig. 4B-C). This finding is in line with the observation that TERRA is necessary for recombination at telomeres in budding yeast (BALK *et al.* 2013). Further, elevated levels of

TERRA are characteristic of human ALT cell lines established from tumors or immortalized *in vitro* (LOVEJOY *et al.* 2012; ARORA *et al.* 2014). TERRA could stabilize D-loop structures to facilitate recombination between telomeres (BALK *et al.* 2013; BALK *et al.* 2014). Given the recent evidence suggesting that ncRNAs can drive the physical association between regions of the genome (ENGREITZ *et al.* 2013), it is also possible that telomere-associated TERRA could tether a telomere *in trans*, promoting the proximity between individual telomeres necessary to support recombination. Such a model is consistent with telomere declustering in RNR *ccq1Δ* survivors (Fig. 5). Instead or in addition, TERRA transcription could promote an increase in telomere mobility to support telomere-telomere interactions necessary for recombination (ARORA *et al.* 2012). Alternatively, it is possible that telomeric R-loops driven by TERRA production promote break-induced replication, a mechanism recently suggested to facilitate telomere maintenance in ALT cells (DILLEY *et al.* 2016), although the genetic requirement for Rad51 in the maintenance of linear chromosomes in *ccq1Δ* survivors is inconsistent with this model (MIYOSHI *et al.* 2008; TOMITA AND COOPER 2008). While discriminating between these explicit molecular mechanisms will require further study, our data clearly support a model in which spontaneous derepression of TERRA plays a critical role in emergence of survivors in the absence of Ccq1.

Distinct roles of TERRA in the presence or absence of telomerase

The effect that TERRA has on telomere length regulation varies, in part depending on the presence or absence of telomerase (AZZALIN AND LINGNER 2008; SCHOEFTNER AND BLASCO 2008; REDON *et al.* 2010; PFEIFFER AND LINGNER 2012; BALK *et al.* 2013; CUSANELLI *et al.* 2013; REDON *et al.* 2013). In addition, our recent work revealed that TERRA molecules in fission yeast can be further grouped into at least two subsets: one is poly(A)+ TERRA, which loses all telomeric tracts and is soluble in the nucleoplasm; the other is poly(A)- TERRA, which has G-rich telomeric sequences, and is bound at telomeric DNA (MORAVEC *et al.* 2016). While poly(A)+ TERRA stimulates telomerase recruitment in telomerase-positive cells (MORAVEC *et al.* 2016), here we demonstrate that poly(A)- TERRA (or G-rich TERRA) promotes telomere recombination in cells with insufficient telomerase function. Therefore, these two subsets of TERRA molecules maintain telomeres through different mechanisms according to the cellular context. Interestingly, expression of “a transcriptionally inducible telomere” cannot prevent *ccq1Δ* cell senescence, and in fact precipitates a more rapid growth crisis in pre-senescent cells (Fig. 3H-J). This observation is consistent with the idea that increased TERRA production can be deleterious to telomere maintenance in some contexts (BALK *et al.* 2013). We note, however, that the tiTEL predominantly produces poly(A)+ TERRA and that nascent TERRA is limited to a single telomere; thus the tiTEL system may model the role for TERRA in telomerase-dependent (MORAVEC *et al.* 2016) but not recombination-dependent telomere maintenance.

TERRA dependent and independent recombination-based telomere maintenance

The “addiction” of *ccq1Δ* survivors to telomere-associated TERRA (suggested by the ability of Rnh201 over-expression to induce a second growth crisis) appears to represent only one potential mode of telomerase-independent telomere maintenance, as these cells also ultimately form a new type of linear, RNase H2-resistant *ccq1Δ* survivor. This mechanism is necessarily distinct from so-called HAATI survivors, which replace the telomeric repeats with “generic” heterochromatin, as this pathway requires the presence of Ccq1 (JAIN *et al.* 2010). What changes might support a productive, TERRA-independent telomere recombination mechanism that can maintain telomeres in the absence of Ccq1? Our data suggest that these RHR *ccq1Δ*

survivors display altered recruitment of telomere binding proteins, including loss of Rap1 (but not Taz1) from the telomere (Fig. 6). This result is somewhat surprising, as Taz1 binds directly to Rap1 and promotes its recruitment to the telomere in fission yeast, thereby bridging the double-stranded telomeric repeat region to Poz1 and the shelterin components that associate with the single-stranded telomeric overhang (CHIKASHIGE AND HIRAOKA 2001; KANOH AND ISHIKAWA 2001; PAN *et al.* 2015). Moreover, loss of Taz1 and phenocopy one another with respect to increased telomere length and de-repression of TERRA (MILLER *et al.* 2005; BAH *et al.* 2012; GREENWOOD AND COOPER 2012), although the mechanisms at play may be distinct (MILLER *et al.* 2005; DEHE *et al.* 2012). We note, however, that recent evidence supports allosteric regulation of Rap1 binding to Tpz1-Poz1 to regulate telomere lengthening (KIM *et al.* 2017), suggesting that the Rap1-Taz1 interface may also be subject to modulation. Further studies will be required to test if changes in the composition and/or conformation of shelterin are tied to the mechanisms allowing for telomere maintenance in the absence of RNA-DNA hybrids.

Importantly, loss of Rap1 is not simply a consequence of these mechanisms that support telomere maintenance in RHR *ccq1Δ* survivors, because deletion of Rap1 is sufficient to make *ccq1Δ* survivors insensitive to the degradation of RNA-DNA hybrids. How Rap1 eviction from the telomeres promotes the maintenance of linear chromosomes in the absence of telomere-associated TERRA is not yet clear, although we have ruled out the participation of telomerase (Supplemental Figure S4D). Decreased Rap1 association could weaken the association of telomeres with the nuclear envelope, which has been suggested to repress telomere recombination in budding yeast (SCHOBER *et al.* 2009). Indeed, Rap1 phosphorylation results in release of telomeres from the inner nuclear membrane in mitosis (FUJITA *et al.* 2012); however, we note that we do not observe any visual changes in the mobility of Rap1 by SDS-PAGE/Western blot in RHR survivors (Figure 6D), which can be discerned in mitotic cells (FUJITA *et al.* 2012). One clue may be that RHR *ccq1Δ* survivors display altered cytological features, including a substantial expansion of the telomere volume (as visualized by Taz1-GFP; Fig. 5). This could reflect a role for Rap1 in maintaining chromosome ends in discrete foci; indeed, Rap1 is required for telomere clustering in budding yeast (MORADI-FARD *et al.* 2016). Alternatively (or in addition), the expansion in telomere volume could reflects weakened telomeric sister chromatid cohesion; in mammalian cells loss of cohesion between sister telomeres has been shown to drive an increase in telomere recombination (RAMAMOORTHY AND SMITH 2015), which could promote telomerase-independent telomere maintenance.

Conclusion

Here we demonstrate that increased TERRA production is a spontaneous, key step in the adoption of recombination-based telomere maintenance in fission yeast, which coincides with an increase in recruitment of Taz1-GFP to the telomere. G-rich TERRA engages at telomeres as RNA-DNA hybrids and promotes telomere recombination in post-senescent *ccq1*Δ survivors. While degradation of this TERRA pool is sufficient to compromise cell growth, ultimately these *ccq1*Δ cells adopt an alternative mechanism to promote the maintenance of linear chromosomes, which we find is characterized by loss of telomeric Rap1. Engineered deletion of Rap1 promotes the efficient formation of RHR survivors, suggesting that altered Rap1 recruitment RHR survivor formation. These findings provide important clues to understanding the generation and maintenance of ALT-positive tumor cells.

Materials and Methods

S. pombe strain generation and culture conditions

S. pombe strains are described in Supplementary Table S1. Standard manipulations and cell culturing were carried out as described (MORENO *et al.* 1991). C-terminal GFP or mCherry tagging was performed with the pFa6a-GFP-kanMX6 or pFa6a-mCherry-kanMX6 cassette (BÄHLER *et al.* 1998; SNAITH *et al.* 2005). pFa6a-natMX6-nmt41-HA was used to tag Rnh201 at the N-terminus as established (BÄHLER *et al.* 1998). In the strain with "transcriptionally inducible" telomere (tiTEL), the thiamine repressible *nmt1*+ gene promoter (*Pnmt1*) was inserted 91 base pairs upstream of the endogenous TERRA transcription start site at Chr I-R (MORAVEC *et al.* 2016). A C-terminal GFP cassette was further integrated after the Taz1 ORF in this tiTEL strain (Strain MKSP1722). Fresh pre-senescent *ccq1*Δ or *trt1*Δ cells were obtained from cross-dissection with telomerase-positive cells. All strains generated by cassette integration were confirmed by PCR. After genetic crosses, progeny were tested by the segregation of markers, PCR, or presence of the relevant fluorescent protein fusion, as appropriate.

S. pombe were grown at 30°C, in yeast extract medium supplemented with amino acids (YE5S) or Edinburgh minimal medium with amino acids (EMM5S). To increase TERRA production, 30 µg/ml Trichostatin A (Cayman Chemical) was added to YE5S or EMM5S media. To suppress the *nmt1*+ or *nmt41*+ gene promoter (MAUNDRELL 1990), 5 µg/ml thiamine (Sigma-Aldrich) was added to EMM5S medium.

Serial culturing

Single colonies from plates were inoculated in liquid medium, and 24 hours later, cell densities were measured using Moxi-Z mini cell counter (ORFLO). Approximately 28 generations were estimated from a single, germinated cell growing on solid medium for 20 generations to generate a colony, followed by a single overnight culture. Cell cultures were measured for their cell densities and diluted to $5x10^5$ cells/ml with fresh medium every 24 hours. At each indicated time point, cells were collected for further analysis or subjected to imaging accordingly. The increase in generations each day were calculated as $\log_2([\text{cell density}]/(5x10^5))$. Growth curves were plotted using GraphPad Prism 7.01.

TeloPCR and length analysis

Experiments and analysis were carried out as described (BENNETT *et al.* 2016; MORAVEC *et al.* 2016). Telomere sequences were amplified after the telomere ends were either ligated to an anchoring primer or extended by oligo d(C) (Telo-PCR). PCR products were purified and subjected to high-throughput sequencing. Telomere lengths were analyzed from sequencing data as described (BENNETT *et al.* 2016). Telomere lengths were also determined by running the Telo-PCR products on a long agarose gel for more than 1 hour, and then the gel was imaged on VerSaDoc imaging system (Bio-Rad). The profile of each lane was analyzed in the software Quantity One 4.6.9.

Live cell imaging and analysis

Cells for imaging were exponentially grown in YE5S or EMM5S media supplemented with adenine hemi sulfate (0.25 mg/mL). Cells in liquid culture were concentrated and applied to glass slides bearing agarose pads (1.4% agarose in EMM). Samples were sealed under a glass coverslip with VALAP (equal parts by weight: Vaseline, lanolin, and paraffin). Images were acquired on an Applied Precision (now GE Healthcare) Deltavision high performance wide field microscope with solid-state illumination and a Photometrics Evolve 512 EMCCD camera. For imaging of Taz1-GFP in Fig. 2C-E and Fig. S4B, each field was captured as a 12 section Z-stack of sample thickness 4.80 µm (optical sectioning every 0.40 µm; this is sufficient to capture

the entire nuclear volume to ensure all telomeric foci are visualized); EMCCD Gain = 100; GFP at 10% power, 100 ms exposure. For telomere volume reconstruction (Fig. 5; Fig. S5E), each field was captured as a 25 section Z-stack of sample thickness 5.0 µm (optical sectioning spacing every 0.2 µm); EMCCD Gain = 100; GFP at 10% power, 50 ms exposure. For cells expressing Rap1-GFP (Fig. 6A; Fig. S4C,D) each field was captured as a 24 section Z-stack of sample thickness 4.80 µm (optical sectioning every 0.2 µm; EMCCD Gain = 200; GFP at 10% power, 25 ms exposure. For visualization of Taz1-GFP and Rad52-mCherry (Fig. 1C; Fig. S5C) each field was captured as a 12 section Z-stack of sample thickness 4.8 µm (optical sectioning spacing every 0.4 µm); EMCCD Gain = 100; GFP at 10% power, 50 ms exposure; mCherry at 10% power, 500 ms exposure. Only live, non-mitotic cells that had completed cytokinesis were considered for Taz1-GFP and cell length analysis. To image mitotic cells (Fig. S1B), Taz1-GFP *ccq1Δ* cells from growth assay end-point (survivor) glycerol stocks were recorded for durations of 1 hour, with a time-lapse of 30 seconds using autofocusing and the same sectioning conditions.

Images were analyzed in ImageJ (Fiji). To calculate the number of Taz1-GFP foci per cell or examine the co-localization of Taz1-GFP and Rad52-mCherry, maximum Z-projections were generated. For quantitative measurement of Taz1-GFP recruitment to telomeres, the intensity of each Taz1-GFP focus was measured from mean intensity projections as the integrated pixel density of the visibly occupied area. The background GFP signal was removed from measurement of each focus by subtracting the integrated density of an empty area of the same size as the focus within the nucleoplasm of the same cell. The intensities of all foci were then summed to give a single measurement per cell.

Real-time PCR to measure TERRA levels

RT-PCR protocols were adapted from previous report (BAH *et al.* 2012). Total RNA was extracted using MasterPure yeast RNA purification kit (Epicentre). To completely eliminate DNA contamination, RNA was treated three times with RNase-free DNase I (provided with the kit). cDNA was generated using SuperScript III (Invitrogen). Each 20 µl reverse transcription reaction contained 5 µg total RNA, 1 µl 10 µM oligo for total TERRA (Sp C-rich telo: 5'-TGTAACCGTGTAACCACGTAACCTTGTAACCC-3') and 1 µl 1 µM reverse control oligo for actin (Sp ACT1(2): 5'-CATCTGTTGGAAAGTAGAAAGAGA AGCAAG-3'), or 2 µl 40 µM oligo(dT) (in the case of poly(A)+ TERRA), 1 µl 10 mM dNTP, 4 µl 5xFirst-Strand Buffer, 2 µl 0.1 M DTT and 1 µl SuperScript III RT enzyme. The reaction was incubated at 50°C for 1 hour and the remaining RNA was degraded by RNase H (NEB) and RNase A (Sigma-Aldrich) by incubating at 37°C for 20 minutes. Real-time PCR was performed on C1000 Touch Thermal Cycler (Bio-Rad), using FastStart Universal SYBR Green Master (Rox) (Roche). For TERRA PCR amplification, each 20 µl reaction contained 2 µl of cDNA, 1 µl of each 10 µM primer (SpRACE290-320_4: 5'-GGGCCCAATAGTGGGGGCATTGTATTTGTG-3'; Sp-subtelo_425: 5'-GAAGTTCACTCAGTCATAATTAATTGGGTAACGGAG-3'). For actin PCR amplification, each 20 µl reaction contained 2 µl of 1:10 diluted cDNA, 1 µl of each 10 µM primer (SpACT1FOR2: 5'-CCGGTATTCATGAGGCTACT-3'; SpACT1REV2: 5'-GGAGGAGCAACAATCTTGAC-3').

qPCR steps: 1 cycle of 95°C-5 min; 45 cycles of 95°C-10 sec and 60°C-30 sec; followed by melting curve. Relative TERRA levels were calculated for each sample after normalization against actin using the ΔΔCt method. Ct values for each reaction were determined using the software Bio-Rad CFX Manager 2.1. Duplicate Ct values were averaged in each run. Each RNA sample was reverse-transcribed into cDNA twice, and each cDNA sample was analyzed by real-time PCR at least three times. Ct values of the same sample were averaged and plotted in GraphPad Prism 6. No RT and no template reactions were always included to control for DNA contaminations.

Real-time PCR to measure Taz1 mRNA levels

Cells were collected at exponential phase and total RNAs were extracted using MasterPure yeast RNA purification kit (Epicentre). Reverse-transcription was performed using M-MuLV RT (NEB) and oligo d(T). We followed standard protocol, 1 µg total RNA was used for each reaction. The same qPCR program was used as above (primers: Taz1 qPCR For: 5'-ACAGGCTTCGTGAGCGAGTT-3'; Taz1 qPCR Rev: 5'-CTCGGACGCGTCACTCTCAT-3')

Southern blots

Experiments were performed as described (BENNETT *et al.* 2016). Briefly, genomic DNA (25 µg) was digested with EcoRI-HF (NEB) at 37°C overnight, electrophoresed on a 1% agarose gel, denatured and transferred to Zeta-Probe GT membrane (Bio-Rad), then hybridized with a telomere-DIG probe in ExpressHyb Solution (Clontech). After hybridization, the membrane was washed and incubated with anti-DIG-AP conjugate (the same kit, 1:1000 dilution). The blot was then treated with SuperSignal West Femto Maximum Sensitivity Kit (ThermoFisher/Pierce), and imaged on VerSaDoc imaging system (Bio-Rad) using the software Quantity One 4.6.9.

Chromatin Immunoprecipitation (ChIP)

ChIP of Rap-GFP expressing cells was carried out as described previously (LORENZI *et al.* 2015) with the following modifications. 75 OD of yeast cells at an of OD_{600} 0.6–1.0 were cross-linked in 1% formaldehyde for 30 min prior to quenching with glycine. Cross-linked material was washed in ice-cold PBS and resuspended in 1ml lysis buffer (50 mM HEPES-KOH pH 7.5, 140 mM NaCl, 1 mM EDTA, 1% Triton X-100, 0.1% sodium deoxycholate, protease inhibitor cocktail (Roche)). Cells were transferred to 1.5 ml screw-cap tubes and subjected to mechanical lysis with silica beads (0.5 mm diameter, BioSpec) using the Mini-BeadBeater-16 instrument (BioSpec), shaking 1 min 30 sec for 6 - 8 times with 3 min intervals. Lysates were centrifuged for 30 min at 16,000xg, and pellets were re-suspended in 500 µl lysis buffer and subjected to sonication using the S-4000 sonicator (Misonix) for 15 min (Amplitude 4, 5 sec pulse with 15 sec cool-down intervals). After centrifugation at 10,000xg for 15 min, the supernatant containing DNA fragments was collected. Lysis buffer with protease inhibitor cocktail (Roche) was added to adjust the volume to about 1.4 ml with 120 µl taken as the input sample. Immunoprecipitations were performed on a rotating wheel at 4°C overnight with GFP-Trap beads (Chromotek). Then the beads were washed 4 times with lysis buffer, lysis buffer plus 500 mM NaCl, wash buffer (10 mM Tris-HCl pH 7.5, 0.25 M LiCl, 0.5% NP40, 0.5% sodium deoxycholate), and lysis buffer respectively. Immunoprecipitated chromatin was eluted by adding 120 µl elution buffer (1% SDS, 100 mM $NaHCO_3$, 40 ug/ml RNase A) and incubated at 37°C for 1 h. The input sample was treated in parallel by adding 6 µl of 20% SDS, 11 µl of 1 M $NaHCO_3$ and RNase A. Cross-links were reversed at 65°C over-night (16 hrs) and DNA was purified using a PCR purification kit (Qiagen). DNA content were quantified by real-time PCR using iTaq Universal SYBR Green Supermix (Bio-Rad) on a C1000 Thermal Cycler instrument (Bio-Rad) with primers: subtel-for (5'-TATTTCTTTATTCAACTTACCGCACTTC-3') and subtel-rev (5'-CAGTAGTGCAGTGTATTATGATAATTAAAATGG-3').

Western blots

Experiments were carried out as described (LORENZI *et al.* 2015). Cells were collected at exponential phase and samples were prepared by TCA precipitation. Antibodies were as follows: a rabbit polyclonal anti-Rap1 and a rabbit polyclonal anti-Taz1 antibody (kind gifts from J. Kanoh and J. P. Cooper, respectively); and a mouse monoclonal anti-beta actin antibody (mAbcam 8224) used as loading control.

DNA immunoprecipitation

Log phase cells were harvested, washed with water, and flash frozen in liquid nitrogen. The frozen pellet was resuspended in 1 ml of RA1 buffer (Macherey-Nagel) supplemented 1% β-mercaptoethanol. The cell suspension was mixed with 300 µl of phenol:chloroform:isoamyl alcohol (25:24:1 saturated with 10 mM Tris-Cl pH 8.0, 1 mM EDTA) and 100 µl of acid washed glass beads. Cells were lysed by mechanical shaking using a cell disruptor (Disruptor Gene) for 3 minutes using the 30 second on/off mode at power 4. Cell extracts were centrifuged (13,000*g*, 20 min, 4 °C). Pellets were washed with 70% ethanol, air-dried, and re-suspended in 200 µl of Tris-EDTA and sonicated with a Bioruptor (Diagenode) to obtain 100–500 bp long fragments. Ten micrograms of sheared nucleic acids were diluted in 1 ml of IP buffer (0.1% SDS, 1% Triton X-100, 10 mM HEPES pH 7.7, 0.1% sodium deoxycholate, 275 mM NaCl) and incubated overnight on a rotating wheel at 4 °C in presence of 1 µg of S9.6 antibody (Kerafast) and 20 µl of protein G sepharose beads (GE Healthcare) blocked with *Escherichia coli* DNA and bovine serum albumin. Beads were washed four times with IP buffer and bound nucleic acids were isolated using the Wizard SV gel and PCR clean-up kit (Promega). Collected DNA fragments were quantified using RT-PCR as described above with the following primers: oF1 (5'-GAAGTTCACTCAGTCATAATTAATTGGGTAACGGAG-3') and oR1 (5'-GGGCCCAATAGTGGGGGCATTGTATTTGTG-3').

Methyl methanesulfonate (MMS) sensitivity assay

Circular survivors in fission yeast are exquisitely sensitive to DSB-inducing agents (JAIN *et al.* 2010), therefore the growth on YE5S plates with methyl methanesulfonate (MMS) can be used to distinguish linear from circular survivors. Cells were first grown in YE5S medium until saturation, then diluted to $1x10^7$ cells/ml, and five additional 5-fold serial dilutions were made. Three microliters of each serial dilution were spotted onto YE5S plates with the presence of 0%, 0.0003% and 0.003% MMS respectively, and grown at 30°C for 2 days prior to imaging.

References:

Abdallah, P., P. Luciano, K. W. Runge, M. Lisby, V. Geli *et al.*, 2009 A two-step model for senescence triggered by a single critically short telomere. Nat Cell Biol 11**:** 988-993.

Apte, M. S., and J. P. Cooper, 2017 Life and cancer without telomerase: ALT and other strategies for making sure ends (don't) meet. Crit Rev Biochem Mol Biol 52**:** 57-73.

Arnoult, N., A. Van Beneden and A. Decottignies, 2012 Telomere length regulates TERRA levels through increased trimethylation of telomeric H3K9 and HP1alpha. Nat Struct Mol Biol 19**:** 948-956.

Arora, R., C. M. Brun and C. M. Azzalin, 2012 Transcription regulates telomere dynamics in human cancer cells. RNA 18**:** 684-693.

Arora, R., Y. Lee, H. Wischnewski, C. M. Brun, T. Schwarz *et al.*, 2014 RNaseH1 regulates TERRA-telomeric DNA hybrids and telomere maintenance in ALT tumour cells. Nat Commun 5**:** 5220.

Azzalin, C. M., and J. Lingner, 2008 Telomeres: the silence is broken. Cell Cycle 7**:** 1161-1165.

Azzalin, C. M., and J. Lingner, 2015 Telomere functions grounding on TERRA firma. Trends Cell Biol 25**:** 29-36.

Azzalin, C. M., P. Reichenbach, L. Khoriauli, E. Giulotto and J. Lingner, 2007 Telomeric repeat containing RNA and RNA surveillance factors at mammalian chromosome ends. Science 318**:** 798-801.

Bah, A., and C. M. Azzalin, 2012 The telomeric transcriptome: from fission yeast to mammals. Int J Biochem Cell Biol 44**:** 1055-1059.

Bah, A., H. Wischnewski, V. Shchepachev and C. M. Azzalin, 2012 The telomeric transcriptome of Schizosaccharomyces pombe. Nucleic Acids Res 40**:** 2995-3005.

Bähler, J., J. Q. Wu, M. S. Longtine, N. G. Shah, A. McKenzie *et al.*, 1998 Heterologous modules for efficient and versatile PCR-based gene targeting in Schizosaccharomyces pombe. Yeast (Chichester, England) 14**:** 943-951.

Balk, B., M. Dees, K. Bender and B. Luke, 2014 The differential processing of telomeres in response to increased telomeric transcription and RNA-DNA hybrid accumulation. RNA Biol 11**:** 95-100.

Balk, B., A. Maicher, M. Dees, J. Klermund, S. Luke-Glaser *et al.*, 2013 Telomeric RNA-DNA hybrids affect telomere-length dynamics and senescence. Nat Struct Mol Biol 20**:** 1199-1205.

Baumann, P., and T. R. Cech, 2001 Pot1, the putative telomere end-binding protein in fission yeast and humans. Science 292**:** 1171-1175.

Beernink, H. T., K. Miller, A. Deshpande, P. Bucher and J. P. Cooper, 2003 Telomere maintenance in fission yeast requires an Est1 ortholog. Curr Biol 13**:** 575-580.

Bennett, H. W., N. Liu, Y. Hu and M. C. King, 2016 TeloPCR-seq: a high-throughput sequencing approach for telomeres. FEBS Lett 590**:** 4159-4170.

Blackburn, E. H., 1991 Structure and function of telomeres. Nature 350**:** 569-573.

Blackburn, E. H., 2001 Switching and signaling at the telomere. Cell 106**:** 661-673.

Buhler, M., and S. M. Gasser, 2009 Silent chromatin at the middle and ends: lessons from yeasts. Embo j 28**:** 2149-2161.

Carneiro, T., L. Khair, C. C. Reis, V. Borges, B. A. Moser *et al.*, 2010 Telomeres avoid end detection by severing the checkpoint signal transduction pathway. Nature 467**:** 228-232.

Cesare, A. J., and R. R. Reddel, 2010 Alternative lengthening of telomeres: models, mechanisms and implications. Nat Rev Genet 11**:** 319-330.

Chikashige, Y., and Y. Hiraoka, 2001 Telomere binding of the Rap1 protein is required for meiosis in fission yeast. Curr Biol 11**:** 1618-1623.

Cooper, J. P., and Y. Hiraoka, 2006 *16 Fission Yeast Telomeres*.

Cooper, J. P., E. R. Nimmo, R. C. Allshire and T. R. Cech, 1997 Regulation of telomere length and function by a Myb-domain protein in fission yeast. Nature 385**:** 744-747.

Cusanelli, E., C. A. Romero and P. Chartrand, 2013 Telomeric noncoding RNA TERRA is induced by telomere shortening to nucleate telomerase molecules at short telomeres. Mol Cell 51**:** 780-791.

de Lange, T., 2005 Shelterin: the protein complex that shapes and safeguards human telomeres. Genes Dev 19**:** 2100-2110.

de Lange, T., 2009 How telomeres solve the end-protection problem. Science 326**:** 948-952.

Dehe, P. M., and J. P. Cooper, 2010 Fission yeast telomeres forecast the end of the crisis. FEBS Lett 584**:** 3725-3733.

Dehe, P. M., O. Rog, M. G. Ferreira, J. Greenwood and J. P. Cooper, 2012 Taz1 enforces cell-cycle regulation of telomere synthesis. Mol Cell 46**:** 797-808.

Deng, Z., J. Norseen, A. Wiedmer, H. Riethman and P. M. Lieberman, 2009 TERRA RNA binding to TRF2 facilitates heterochromatin formation and ORC recruitment at telomeres. Mol Cell 35**:** 403-413.

Dilley, R. L., P. Verma, N. W. Cho, H. D. Winters, A. R. Wondisford *et al.*, 2016 Break-induced telomere synthesis underlies alternative telomere maintenance. Nature 539**:** 54-58.

El Hage, A., S. L. French, A. L. Beyer and D. Tollervey, 2010 Loss of Topoisomerase I leads to R-loop-mediated transcriptional blocks during ribosomal RNA synthesis. Genes Dev 24**:** 1546-1558.

Engreitz, J. M., A. Pandya-Jones, P. McDonel, A. Shishkin, K. Sirokman *et al.*, 2013 The Xist lncRNA exploits three-dimensional genome architecture to spread across the X chromosome. Science 341**:** 1237973.

Fallet, E., P. Jolivet, J. Soudet, M. Lisby, E. Gilson *et al.*, 2014 Length-dependent processing of telomeres in the absence of telomerase. Nucleic Acids Res 42**:** 3648-3665.

Feuerhahn, S., N. Iglesias, A. Panza, A. Porro and J. Lingner, 2010 TERRA biogenesis, turnover and implications for function. FEBS Lett 584**:** 3812-3818.

Flynn, R. L., R. C. Centore, R. J. O'Sullivan, R. Rai, A. Tse *et al.*, 2011 TERRA and hnRNPA1 orchestrate an RPA-to-POT1 switch on telomeric single-stranded DNA. Nature 471**:** 532-536.

Fujita, I., Y. Nishihara, M. Tanaka, H. Tsujii, Y. Chikashige *et al.*, 2012 Telomere-nuclear envelope dissociation promoted by Rap1 phosphorylation ensures faithful chromosome segregation. Curr Biol 22**:** 1932-1937.

Gotta, M., T. Laroche, A. Formenton, L. Maillet, H. Scherthan *et al.*, 1996 The clustering of telomeres and colocalization with Rap1, Sir3, and Sir4 proteins in wild-type Saccharomyces cerevisiae. J Cell Biol 134**:** 1349-1363.

Graf, M., D. Bonetti, A. Lockhart, K. Serhal, V. Kellner *et al.*, 2017 Telomere Length Determines TERRA and R-Loop Regulation through the Cell Cycle. Cell 170**:** 72-85 e14.

Greenwood, J., and J. P. Cooper, 2012 Non-coding telomeric and subtelomeric transcripts are differentially regulated by telomeric and heterochromatin assembly factors in fission yeast. Nucleic Acids Res 40**:** 2956-2963.

Heidenreich, B., and R. Kumar, 2017 TERT promoter mutations in telomere biology. Mutat Res 771**:** 15-31.

Hoze, N., M. Ruault, C. Amoruso, A. Taddei and D. Holcman, 2013 Spatial telomere organization and clustering in yeast Saccharomyces cerevisiae nucleus is generated by a random dynamics of aggregation-dissociation. Mol Biol Cell 24**:** 1791-1800, s1791-1710.

Huertas, P., and A. Aguilera, 2003 Cotranscriptionally formed DNA:RNA hybrids mediate transcription elongation impairment and transcription-associated recombination. Mol Cell 12**:** 711-721.

Jain, D., A. K. Hebden, T. M. Nakamura, K. M. Miller and J. P. Cooper, 2010 HAATI survivors replace canonical telomeres with blocks of generic heterochromatin. Nature 467**:** 223-227.

Kanoh, J., and F. Ishikawa, 2001 spRap1 and spRif1, recruited to telomeres by Taz1, are essential for telomere function in fission yeast. Curr Biol 11**:** 1624-1630.

Khadaroo, B., M. T. Teixeira, P. Luciano, N. Eckert-Boulet, S. M. Germann *et al.*, 2009 The DNA damage response at eroded telomeres and tethering to the nuclear pore complex. Nat Cell Biol 11**:** 980-987.

Kim, J. K., J. Liu, X. Hu, C. Yu, K. Roskamp *et al.*, 2017 Structural Basis for Shelterin Bridge Assembly. Mol Cell 68**:** 698-714.e695.

Kim, N. W., M. A. Piatyszek, K. R. Prowse, C. B. Harley, M. D. West *et al.*, 1994 Specific association of human telomerase activity with immortal cells and cancer. Science 266**:** 2011-2015.

Leonardi, J., J. A. Box, J. T. Bunch and P. Baumann, 2008 TER1, the RNA subunit of fission yeast telomerase. Nat Struct Mol Biol 15**:** 26-33.

Longhese, M. P., D. Bonetti, N. Manfrini and M. Clerici, 2010 Mechanisms and regulation of DNA end resection. Embo j 29**:** 2864-2874.

Lorenzi, L. E., A. Bah, H. Wischnewski, V. Shchepachev, C. Soneson *et al.*, 2015 Fission yeast Cactin restricts telomere transcription and elongation by controlling Rap1 levels. Embo j 34**:** 115-129.

Lovejoy, C. A., W. Li, S. Reisenweber, S. Thongthip, J. Bruno *et al.*, 2012 Loss of ATRX, genome instability, and an altered DNA damage response are hallmarks of the alternative lengthening of telomeres pathway. PLoS Genet 8**:** e1002772.

Luke, B., A. Panza, S. Redon, N. Iglesias, Z. Li *et al.*, 2008 The Rat1p 5' to 3' exonuclease degrades telomeric repeat-containing RNA and promotes telomere elongation in Saccharomyces cerevisiae. Mol Cell 32**:** 465-477.

Lundblad, V., and E. H. Blackburn, 1993 An alternative pathway for yeast telomere maintenance rescues est1- senescence. Cell 73**:** 347-360.

Maestroni, L., J. Audry, S. Matmati, B. Arcangioli, V. Geli *et al.*, 2017 Eroded telomeres are rearranged in quiescent fission yeast cells through duplications of subtelomeric sequences. Nat Commun 8**:** 1684.

Maicher, A., L. Kastner, M. Dees and B. Luke, 2012 Deregulated telomere transcription causes replication-dependent telomere shortening and promotes cellular senescence. Nucleic Acids Res 40**:** 6649-6659.

Mandell, J. G., J. Bahler, T. A. Volpe, R. A. Martienssen and T. R. Cech, 2005 Global expression changes resulting from loss of telomeric DNA in fission yeast. Genome Biol 6**:** R1.

Maundrell, K., 1990 nmt1 of fission yeast. A highly transcribed gene completely repressed by thiamine. The Journal of biological chemistry 265**:** 10857-10864.

Miller, K. M., M. G. Ferreira and J. P. Cooper, 2005 Taz1, Rap1 and Rif1 act both interdependently and independently to maintain telomeres. Embo j 24**:** 3128-3135.

Miyoshi, T., J. Kanoh, M. Saito and F. Ishikawa, 2008 Fission yeast Pot1-Tpp1 protects telomeres and regulates telomere length. Science 320**:** 1341-1344.

Moradi-Fard, S., J. Sarthi, M. Tittel-Elmer, M. Lalonde, E. Cusanelli *et al.*, 2016 Smc5/6 Is a Telomere-Associated Complex that Regulates Sir4 Binding and TPE. PLoS Genet 12**:** e1006268.

Moravec, M., H. Wischnewski, A. Bah, Y. Hu, N. Liu *et al.*, 2016 TERRA promotes telomerase-mediated telomere elongation in Schizosaccharomyces pombe. EMBO Rep 17**:** 999-1012.

Moreno, S., A. Klar and P. Nurse, 1991 Molecular genetic analysis of fission yeast Schizosaccharomyces pombe. Methods in enzymology 194**:** 795-823.

Moser, B. A., Y. T. Chang, J. Kosti and T. M. Nakamura, 2011 Tel1ATM and Rad3ATR kinases promote Ccq1-Est1 interaction to maintain telomeres in fission yeast. Nat Struct Mol Biol 18**:** 1408-1413.

Nakamura, T. M., J. P. Cooper and T. R. Cech, 1998 Two modes of survival of fission yeast without telomerase. Science 282**:** 493-496.

Nakamura, T. M., G. B. Morin, K. B. Chapman, S. L. Weinrich, W. H. Andrews *et al.*, 1997 Telomerase catalytic subunit homologs from fission yeast and human. Science 277**:** 955-959.

Nandakumar, J., and T. R. Cech, 2013 Finding the end: recruitment of telomerase to telomeres. Nat Rev Mol Cell Biol 14**:** 69-82.

O'Sullivan, R. J., N. Arnoult, D. H. Lackner, L. Oganesian, C. Haggblom *et al.*, 2014 Rapid induction of alternative lengthening of telomeres by depletion of the histone chaperone ASF1. Nat Struct Mol Biol 21**:** 167-174.

Pan, L., K. Hildebrand, C. Stutz, N. Thoma and P. Baumann, 2015 Minishelterins separate telomere length regulation and end protection in fission yeast. Genes Dev 29**:** 1164-1174.

Pfeiffer, V., and J. Lingner, 2012 TERRA promotes telomere shortening through exonuclease 1-mediated resection of chromosome ends. PLoS Genet 8**:** e1002747.

Pitt, C. W., and J. P. Cooper, 2010 Pot1 inactivation leads to rampant telomere resection and loss in one cell cycle. Nucleic Acids Res 38**:** 6968-6975.

Porro, A., S. Feuerhahn, J. Delafontaine, H. Riethman, J. Rougemont *et al.*, 2014 Functional characterization of the TERRA transcriptome at damaged telomeres. Nat Commun 5**:** 5379.

Ramamoorthy, M., and S. Smith, 2015 Loss of ATRX Suppresses Resolution of Telomere Cohesion to Control Recombination in ALT Cancer Cells. Cancer Cell 28**:** 357-369.

Redon, S., P. Reichenbach and J. Lingner, 2010 The non-coding RNA TERRA is a natural ligand and direct inhibitor of human telomerase. Nucleic Acids Res 38**:** 5797-5806.

Redon, S., I. Zemp and J. Lingner, 2013 A three-state model for the regulation of telomerase by TERRA and hnRNPA1. Nucleic Acids Res 41**:** 9117-9128.

Rippe, K., and B. Luke, 2015 TERRA and the state of the telomere. Nat Struct Mol Biol 22**:** 853-858.

Ruault, M., A. De Meyer, I. Loiodice and A. Taddei, 2011 Clustering heterochromatin: Sir3 promotes telomere clustering independently of silencing in yeast. J Cell Biol 192**:** 417-431.

Schober, H., H. Ferreira, V. Kalck, L. R. Gehlen and S. M. Gasser, 2009 Yeast telomerase and the SUN domain protein Mps3 anchor telomeres and repress subtelomeric recombination. Genes Dev 23**:** 928-938.

Schoeftner, S., and M. A. Blasco, 2008 Developmentally regulated transcription of mammalian telomeres by DNA-dependent RNA polymerase II. Nat Cell Biol 10**:** 228-236.

Schreiner, S. M., P. K. Koo, Y. Zhao, S. G. Mochrie and M. C. King, 2015 The tethering of chromatin to the nuclear envelope supports nuclear mechanics. Nat Commun 6**:** 7159.

Shay, J. W., and S. Bacchetti, 1997 A survey of telomerase activity in human cancer. Eur J Cancer 33**:** 787-791.

Shore, D., and A. Bianchi, 2009 Telomere length regulation: coupling DNA end processing to feedback regulation of telomerase. Embo j 28**:** 2309-2322.

Snaith, H. A., I. Samejima and K. E. Sawin, 2005 Multistep and multimode cortical anchoring of tea1p at cell tips in fission yeast. Embo j 24**:** 3690-3699.

Subramanian, L., B. A. Moser and T. M. Nakamura, 2008 Recombination-based telomere maintenance is dependent on Tel1-MRN and Rap1 and inhibited by telomerase, Taz1, and Ku in fission yeast. Mol Cell Biol 28**:** 1443-1455.

Tang, W., R. Kannan, M. Blanchette and P. Baumann, 2012 Telomerase RNA biogenesis involves sequential binding by Sm and Lsm complexes. Nature 484**:** 260-264.

Teixeira, M. T., M. Arneric, P. Sperisen and J. Lingner, 2004 Telomere length homeostasis is achieved via a switch between telomerase- extendible and -nonextendible states. Cell 117**:** 323-335.

Tomita, K., and J. P. Cooper, 2008 Fission yeast Ccq1 is telomerase recruiter and local checkpoint controller. Genes Dev 22**:** 3461-3474.

Tuzon, C. T., B. Borgstrom, D. Weilguny, R. Egel, J. P. Cooper *et al.*, 2004 The fission yeast heterochromatin protein Rik1 is required for telomere clustering during meiosis. J Cell Biol 165**:** 759-765.

Wang, X., and P. Baumann, 2008 Chromosome fusions following telomere loss are mediated by single-strand annealing. Mol Cell 31**:** 463-473.

Webb, C. J., and V. A. Zakian, 2008 Identification and characterization of the Schizosaccharomyces pombe TER1 telomerase RNA. Nat Struct Mol Biol 15**:** 34-42.

Wright, W. E., M. A. Piatyszek, W. E. Rainey, W. Byrd and J. W. Shay, 1996 Telomerase activity in human germline and embryonic tissues and cells. Dev Genet 18**:** 173-179.

Yu, T. Y., Y. W. Kao and J. J. Lin, 2014 Telomeric transcripts stimulate telomere recombination to suppress senescence in cells lacking telomerase. Proc Natl Acad Sci U S A 111**:** 3377-3382.

Acknowledgements
We are indebted to the Yeast Genomic Resource Center (YGRC) at Osaka University for providing access to strains, as well as the many researchers who have deposited strains at this resource. We also thank J. Kanoh and J. P. Cooper for sharing antibodies.

Funding
This work was supported by the New Innovator Award (National Institutes of Health, Office of the Director) - DP2OD008429 (to M.C.K), the Raymond and Beverly Sackler Institute for Biological, Physical, and Engineering Sciences (to M.C.K. and H.W.B.) and the Yale Science, Technology and Research Scholars Program (STARS II) (to H.W.B.).

Figure Legends

Figure 1. Recombination factors are loaded at telomeres shortly after germination. (A) Serial culturing of WT, *ccq1Δ* and *ccq1Δrad55Δ* cells. Plot of cell density versus number of generations since germination with cells diluted once every 24 hours. (B) Box and whiskers plot of telomere length derived from TeloPCR-seq of the indicated genetic background and number of generations. Box is from the 5th-95th percentile with the whiskers showing all data points. The black line indicates the mean. See also Table S1. (C) Telomeres are recognized as DNA damage shortly after germination in *ccq1Δ* cultures. Representative micrographs of *ccq1Δ* cells expressing Taz1-GFP and Rad52-mCherry after 20 generations. The percent of cells with the indicated phenotype are noted. BF = brightfield; Scale Bar = 10 μm (D) The number of Taz1-GFP foci is less in *ccq1Δ* cells than WT cells after 28 generations. $p < 0.0001$ by K-S test.

Figure 2. Telomere association of Taz1-GFP increases over the emergence of *ccq1Δ* survivors. (A) Plots of cell length over the course of the WT Taz1-GFP and *ccq1*Δ Taz1-GFP serial culturing growth assay. (B) Expression of Taz1-GFP does not substantially change the crisis and escape of *ccq1*Δ cells. Southern blot of EcoRI digested genomic DNA from the samples indicated, hybridized with a DIG-labeled telomere probe derived from a cloned telomere and visualized using a biotinylated anti-DIG antibody followed by streptavidin-HRP and chemilluminescence imaging. The contrast was increased to visualize telomere size in the bottom panel. The *ccq1*Δ survivors also have a higher band of ~ 8 kb (marked with an asterisk; this is likely due to the partial loss of the distal EcoRI cutting site at telomere ends, and these telomeres are therefore restricted at the second, upstream EcoRI site instead). (C-D) Taz1-GFP intensity decreases during the growth crisis but is higher than WT in *ccq1Δ* survivors. (C) Fluorescence micrographs of Taz1-GFP in WT cells (left panel) or *ccq1Δ* cells after 20, 150 and >250 generations from the growth assay shown in panel (A). During the crisis (150 generations), the Taz1-GFP signal becomes diffusely nuclear in some cells (asterisk) and telomeric Taz1-GFP signals become declustered (arrow). In *ccq1Δ* survivors, both the focal nature and intensity of Taz1-GFP are restored. Many *ccq1Δ* survivor cells have one very bright Taz1-GFP focus (arrowhead). (D) The summed Taz1-GFP intensity per cell over the course of the growth assay in (A). In WT cells, the intensity of Taz1-GFP remains constant over >250 generations. In *ccq1Δ* cells, Taz1-GFP intensity decreases as cells enter the growth crisis (~95-152 generations) but then recovers and ultimately surpasses the WT intensity level during the emergence of survivors (~181 generations). n>50 cells for each day in (D). (E) The appearance of Taz1-GFP in *ccq1*Δ survivors is the same if Taz1-GFP is integrated after survivor formation. Fluorescence micrographs of *ccq1*Δ survivors from the end of the growth assay shown in Figure 1A after integration of Taz1-GFP. Scale bar = 5 μm

Figure 3. Telomere association of Taz1-GFP correlates with TERRA induction induced spontaneously during *ccq1Δ* survivor emergence or through chemical or engineered mechanisms. (A-C) Telomere-association of Taz1-GFP is promoted by TSA or tiTEL induction and reduced by Rnh201 over-expression. Telomeric Taz1-GFP intensity was quantified as in Fig. 2D. At least 50 cells for each sample, plotted as the mean with SD. (A) An increase in telomere-associated Taz1-GFP is seen 24 hours after treatment with TSA (30 ug/mL). (B) TERRA production from a single telomere is sufficient to increase the level of focal Taz1-GFP intensity per cell. WT Taz1-GFP cells or Taz1-GFP in cells with the nmt1 promoter integrated upstream of the TERRA TSS of telomere I-R (tiTEL) were either repressed (with thiamine) or induced (without thiamine) for 2, 4 or 6 days. (C) TSA increases telomere-associated Taz1-GFP

in repressed nmt41-Rnh201 cells, but this increase is largely reversed upon Rnh201 induction. * p<0.05; ** p<0.01; *** p<0.001; **** p< 0.0001 by Student's t-test with correction for multiple comparisons. (D) TERRA levels are higher in *ccq1Δ* cells shortly after germination and are dramatically increased in survivors. Quantitative RT-PCR analysis for G-rich TERRA normalized to WT cells and plotted as the mean with SD from three replicates. (E) TERRA levels increase concomitant with the emergence of *ccq1Δ* survivors between 152 and 240 generations. Quantitative RT-PCR analysis for both total and poly(A+) TERRA normalized to generation 28 *ccq1Δ* cells and plotted as the mean with SD from three replicates. (F) Telomeric RNA/DNA hybrids increase in *ccq1*Δ survivor cells as assessed by DNA-IP using the S9.6 antibody (see Methods). Mean of three replicates plotted with the standard deviation. * = p < 0.05. (G) Newly germinated *ccq1Δrad55Δ* cells (38 generations) contain high levels of total TERRA but TERRA is depleted in *ccq1Δrad55Δ* survivors as determined by RT-PCR as in (D). (H-I) tiTEL induction leads to a more rapid and pronounced growth crisis in recently germinated *ccq1Δ* cells. (H) Serial restreaking of two *ccq1Δ* tiTEL clones on EMM – thiamine to drive tiTEL induction leads to poorer growth than seen for *ccq1Δ* cells alone. (I) Serial culturing in liquid media reveals poorer growth immediately after germination for *ccq1Δ* tiTEL cells compared to *ccq1Δ* cells, although survivors emerge in both conditions. (J) Increased loading of recombination factors on telomeres in newly germinated *ccq1Δ* tiTEL cells upon induction. Fluorescence micrographs of newly germinated (33 generations) *ccq1*Δ tiTEL cells expressing Taz1-GFP and Rad52-mCherry were quantified for co-localization. ** p<0.01 by Student's t-test.

Figure 4. Degradation of RNA-DNA duplexes restored Taz1-GFP intensity and compromises the growth of *ccq1Δ* survivors. (A) WT or *ccq1Δ* Taz1-GFP survivor cells from the end point of the growth assay in Fig. 2 were modified to insert the nmt41 promoter upstream of the *Rnh201* coding sequence. Images were acquired with and without induction of Rnh201 for 24 hours and telomere-associated Taz1-GFP intensity was measured as in Fig. 2D. ** p<0.01 (B) Rnh201 induction returns *ccq1Δ* survivors into a growth crisis. Strains described in (A) were serially cultured with (repressed) or without (induced) thiamine, as indicated. (C) DIC imaging shows that Rnh201 over-expression leads to a new growth crisis in *ccq1*Δ survivors. The first three days of liquid culturing corresponding to Fig. 4B are shown. Note the increase in cell length, indicating checkpoint arrest. Cell length measured for all four growth conditions evaluated in (B) is plotted at the right. (D) The telomeres of RHR *ccq1Δ* survivors selected after constitutive Rnh201 over-expression are similar in length and structure to the initial *ccq1Δ* survivors. Southern blot of EcoRI digested genomic DNA as in Fig. 2B. The rDNA probe serves as a loading control. (E) Like linear survivors (*ccq1*Δ L), the RHR *ccq1Δ* survivors are not sensitive to MMS, indicating that they maintain linear chromosomes. Circular survivors (*trt1*Δ O) were used as a control; the growth of this strain is impaired on MMS plates, as expected.

Figure 5. *ccq1Δ* survivors that form after constitutive Rnh201 over-expression display increased Taz1-GFP recruitment and have telomeres that appear larger and declustered. (A) Fluorescence imaging of Taz1-GFP reveals changes in telomere appearance upon long-term induction of Rnh201 in *ccq1Δ* Taz1-GFP survivor cells. Fluorescence micrographs of WT or *ccq1Δ* Taz1-GFP survivor cells (end point of the growth assay in Figure 4A) compared to survivors that emerge after long-term Rnh201 over-expression (RHR *ccq1Δ* survivors). (B) The intensity of focal Taz1-GFP increases in *ccq1*Δ Rnh201 over-expressing survivors after long-term induction back to levels similar to initial *ccq1*Δ survivors. Taz1-GFP intensity measured and plotted as in Fig. 2D. (C) Taz1-GFP foci were reconstructed using an algorithm previously developed by our group (see Methods). The mean cross-section width was determined for each

focus; for foci with a cross-section smaller then the point spread function (PSF), the focus will appear with the dimensions of the PSF. Reconstructed WT Taz1-GFP foci (n=352) are nearly all the size of the PSF (170 nm, dashed line) or smaller. While *ccq1Δ* survivors display slightly larger Taz1-GFP foci (n=252), the largest Taz1-GFP foci are seen in the RHR *ccq1Δ* survivors (n=132). The box represent the 25th and 75th quartiles, the mean is the black line and the whiskers include all data. **** $p < 0.0001$ by Student's t-test corrected for multiple comparisons. (D) Representative examples of reconstructed Taz1-GFP foci in the three genetic backgrounds. The raw image is on the left and the telomeric focus is reconstructed on the right. Scale bar = 1 μm.

Figure 6. Loss of Rap1 promotes formation of *ccq1Δ* survivors in the context of constitutive Rnh201 over-expression. (A) Fluorescence imaging of Rap1-GFP reveals decreased recruitment to the telomere upon long-term induction of Rnh201 in *ccq1Δ* survivor cells. Fluorescence micrographs of WT or *ccq1Δ* Rap1-GFP survivor cells after long-term Rnh201 over-expression (RHR *ccq1Δ* survivors). Scale bar = 10 μm (B) Quantification of the number of Rap1-GFP foci after long-term induction of Rnh201 in the WT and *ccq1Δ* backgrounds. At least 200 cells were analyzed. (C) The association of Rap1 with telomeres is also observed upon Rnh201 over-expression by chromatin immunoprecipitation-qPCR. Normalized to WT cells and plotted as the mean with SD from three biological replicates. *** p=0.0002 by Student's t-test. (D) Taz1 levels increase in the absence of Rap1 and in all varieties of *ccq1Δ* survivors while Rap1 levels are unaffected. Whole cell extracts were separated on SDS-PAGE, blotted and probed with antibodies to Taz1, Rap1, or β-actin (as a loading control). (E) Deletion of Rap1 prevents the growth crisis upon Rnh201 over-expression in *ccq1Δ* survivors. Serial culturing of either *ccq1Δ* (top) or *rap1Δccq1Δ* (bottom) nmt41-Rnh201 cells under constitutive repression (black), over-expression (light gray circles), or induced induction of over-expression (OE at day 13, black arrow; dark gray diamonds). Cell density is normalized to the Rnh201-repressed condition.

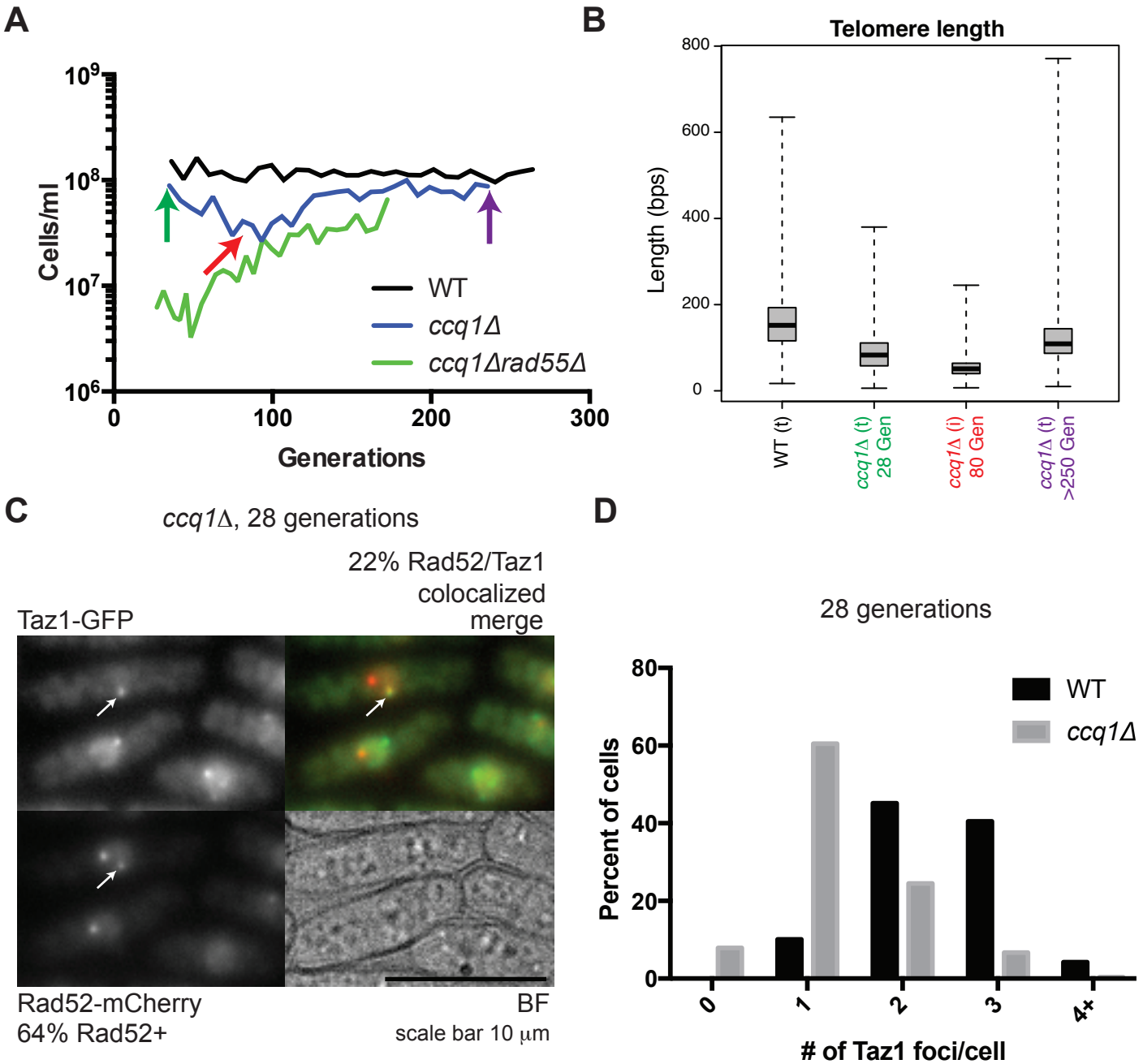

Hu, Figure 1

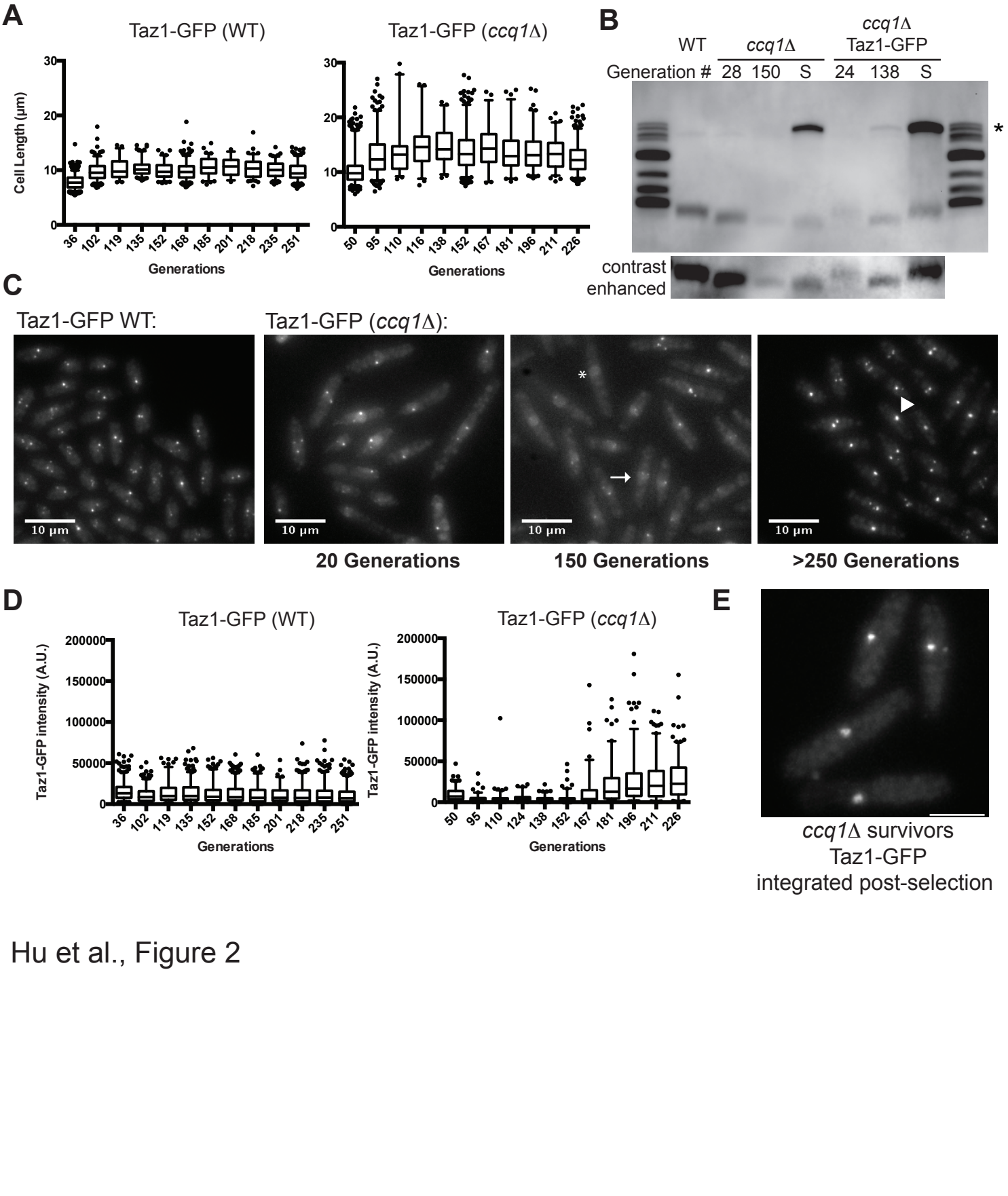

Hu et al., Figure 2

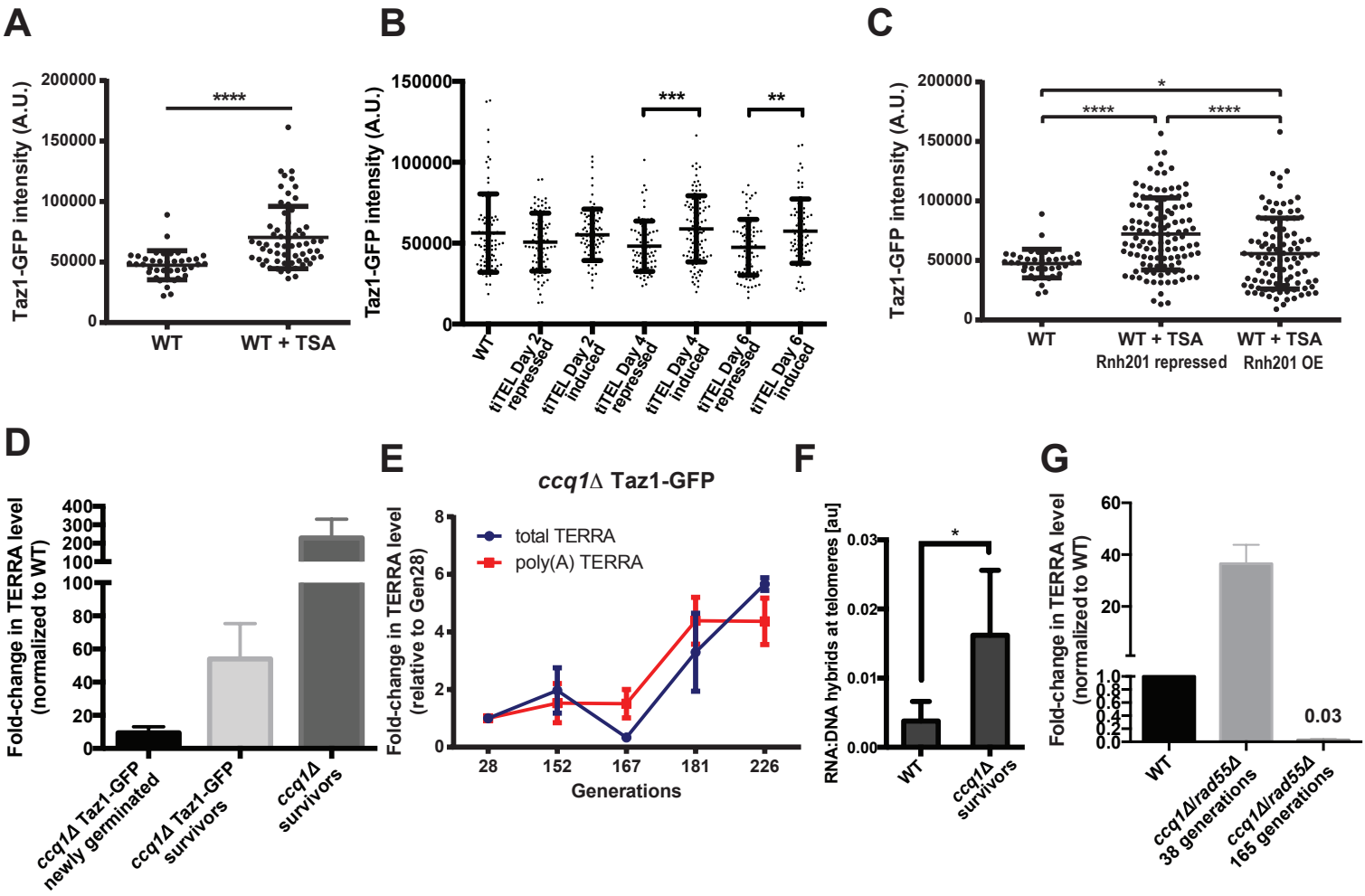

Hu et al., Figure 3

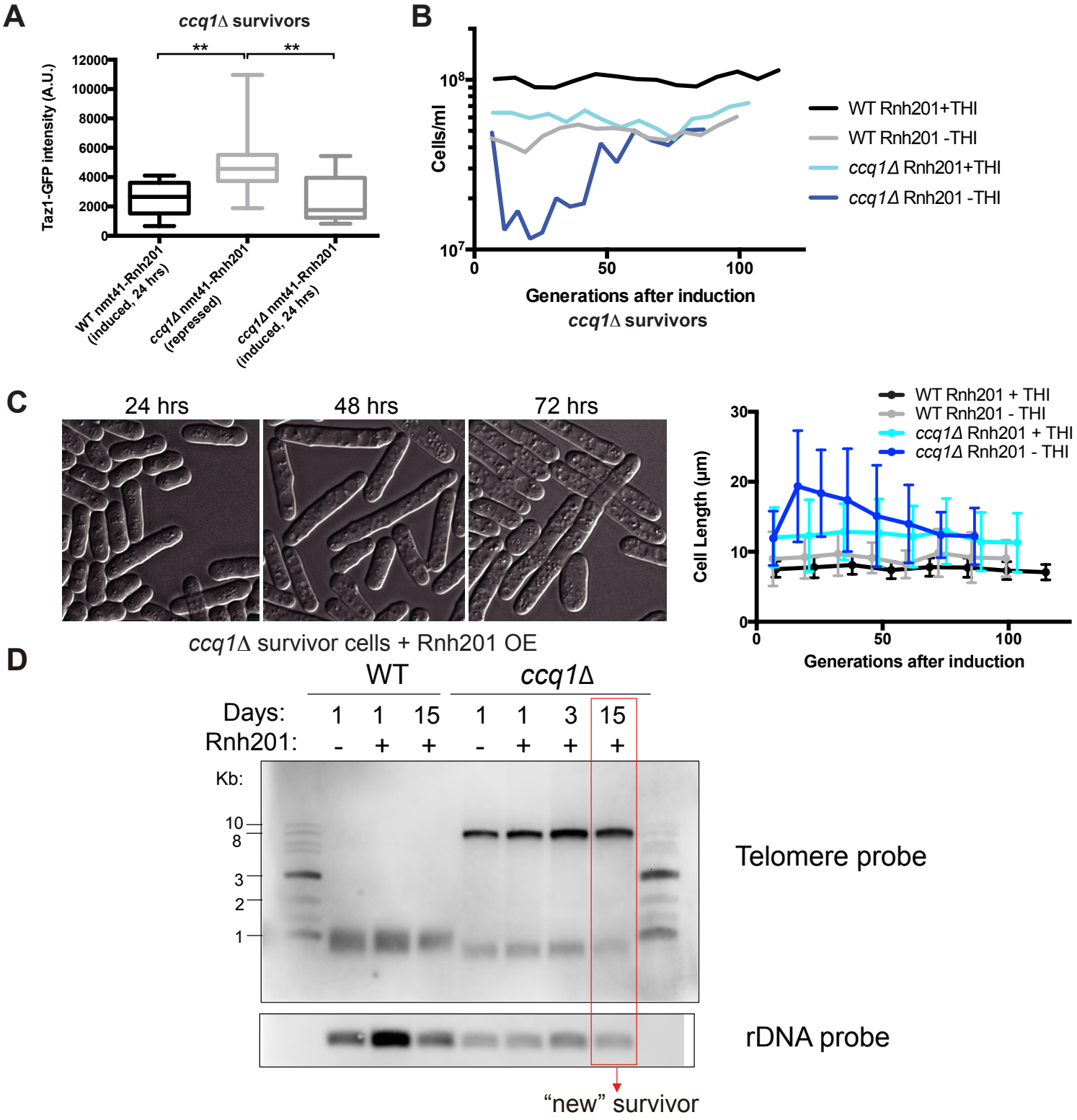

Hu et al., Figure 4

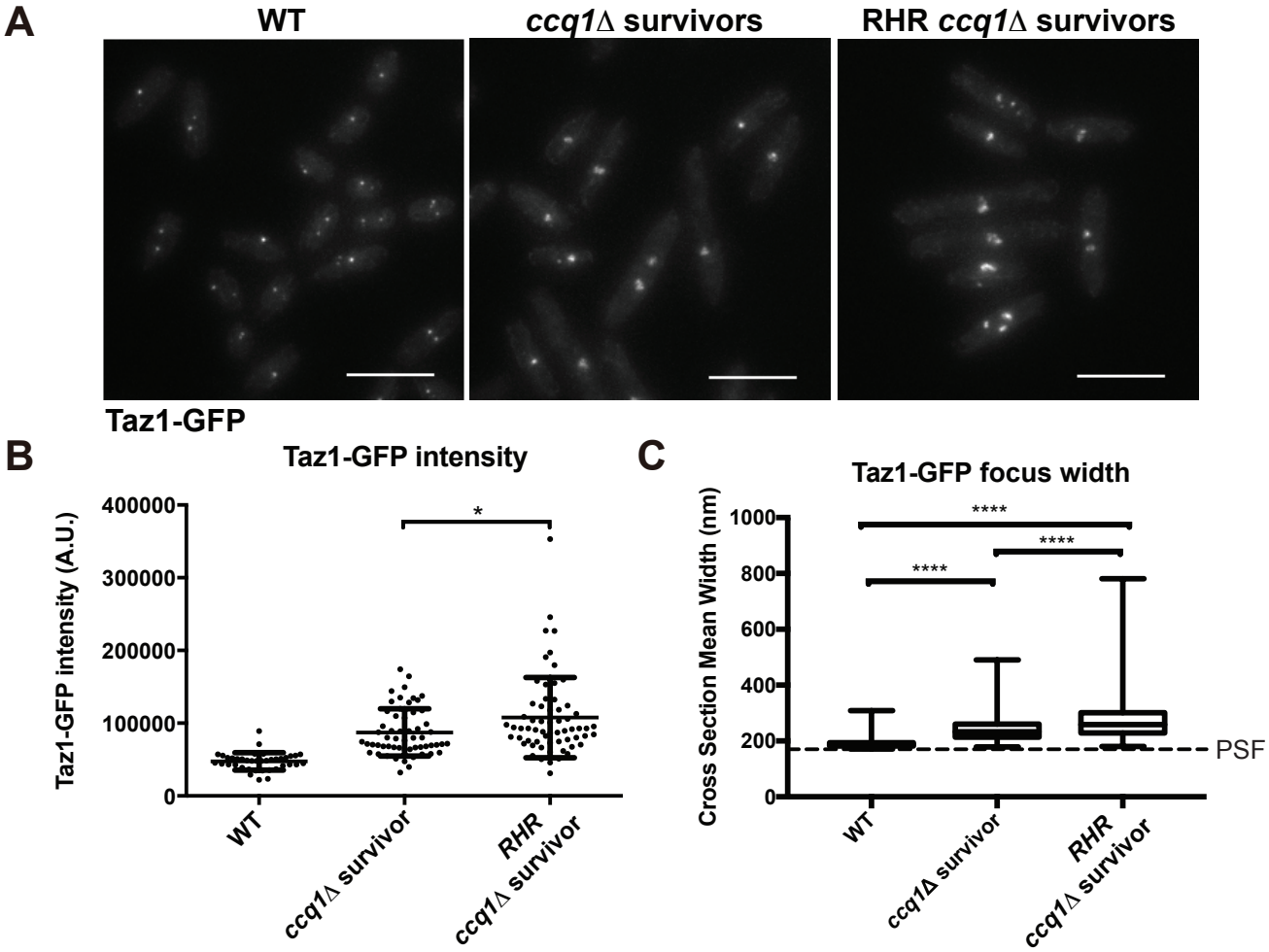

Hu et al., Figure 5

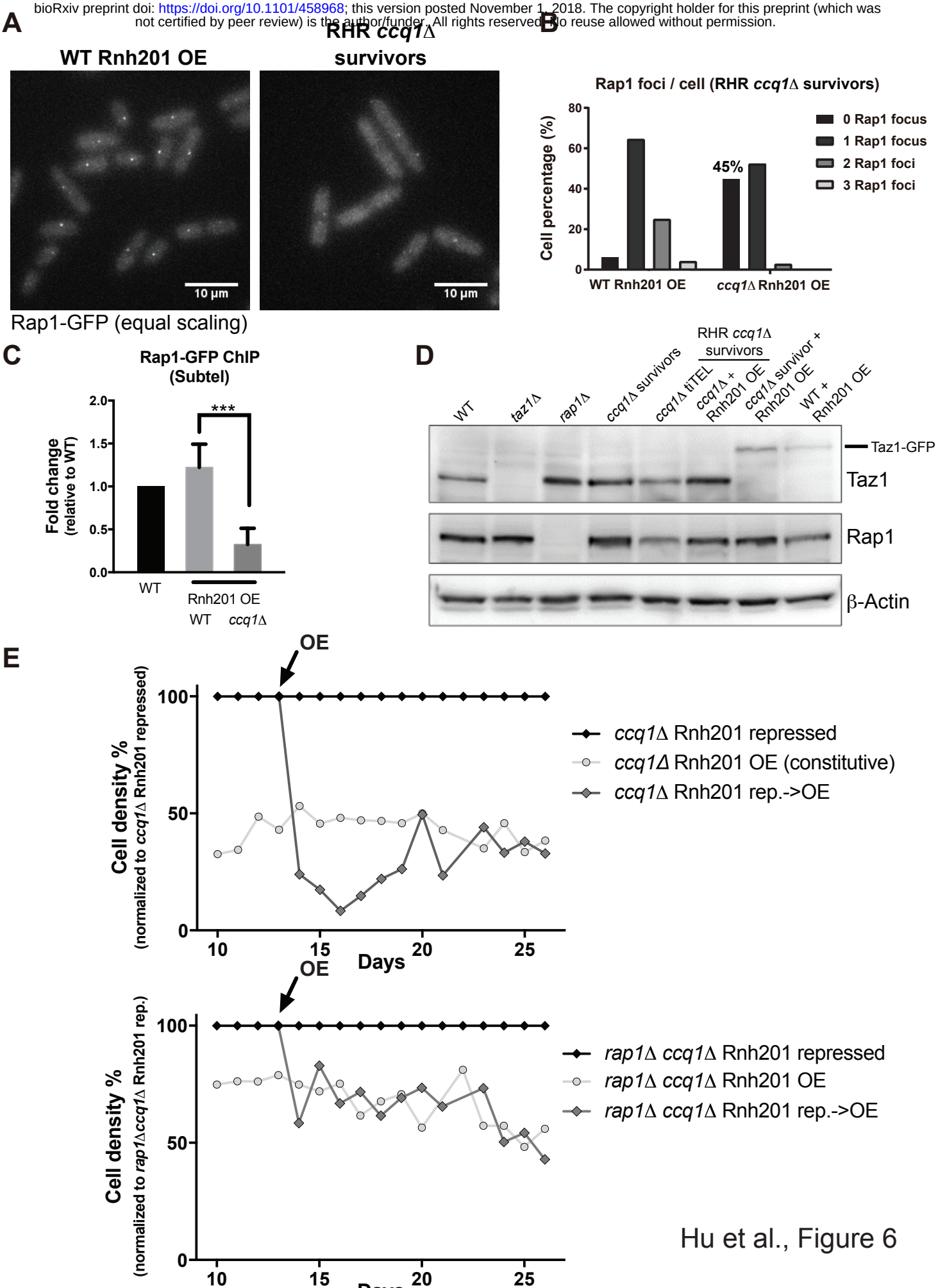

Hu et al., Figure 6